FINAL PUBLISHABLE REPORT

Grant Agreement number	18SIB03
Project short name	BxDiff
Project full title	New quantities for the measurement of appearance

Project start date and duration:		1 May 2019, 42 months
Coordinator: Gaël Obein, CNAM	Tel: +33 158 808 788	E-mail: gael.obein@lecnam.net
Project website address: https://bxdiff.cmi.cz//		
Internal Funded Partners: 1. CNAM, France 2. Aalto, Finland 3. CMI, Czech Republic 4. CSIC, Spain 5. DFM, Denmark 6. METAS, Switzerland 7. PTB, Germany 8. RISE, Sweden	External Funded Partners: 9. DTU, Denmark 10. Innventia, Sweden 11. KU Leuven, Belgium 12. UJM, France	Unfunded Partners: 13. CI, New Zealand 14. Labsphere, United States 15. Lucideon, United Kingdom 16. NCS, Sweden 17. SG, France
RMG: -		

TABLE OF CONTENTS

1 Overview

Product appearance and visual branding are important drivers for consumer purchase decisions, as they underpin perceptions of ‘quality’ and ‘desirability’. The project aimed to advance primary metrology in spectrophotometry to meet industrial needs for the quantitative measurement of appearance. This was accomplished by i) defining new spectrophotometric quantities, ii) taking previously ignored corrections terms into account, and iii) developing new traceable spectrophotometric primary references to provide new tools for quality control and more realistic solutions for virtual prototyping. This research aimed to benefit different industrial sectors like automotive, paper, cosmetic, 3D-printing and virtual reality rendering as well as scientific related applications like aerospace missions.

2 Need

Industry is developing increasingly complex materials that produce visual effects made to look beautiful and appealing (like iridescence or sparkle), or to accomplish a given function (like retroreflection). To develop and control their appearance properties, traditional colorimetry is not adapted anymore, and industrials increasingly start to use bidirectional reflectance measurements in various contexts. Traditional reflectance references based on a single angular measurement configuration will be deemed obsolete in the future. New commercial bidirectional spectrophotometers are diverse, flexible and high performing. National Metrology Institutes (NMIs) must continue supporting the ongoing revolution in spectrophotometry by providing bidirectional reflectance calibration services for angular configurations in addition to the classical 0°:45° configuration. The primary scales kept by participating NMIs have never been compared for e.g. out-of plane angular configurations that are representative of those used in the new generation of commercial products. Furthermore, the influence of common optical phenomena like speckle and polarisation has never been thoroughly studied in Bidirectional Reflectance Distribution Function (BRDF) measurements and might have a non-neglecting effect in uncertainty budgets.

The appearance of objects depends not only on the material(s), colour, shape and lighting environment, but also on the observation distance and object size. Therefore, the optical properties of materials must be measured at different scales: from the macroscopic to the microscopic.

Bidirectional Transmittance Distribution Function (BTDF) as a quantity, is the angle dependent radiance in transmission, referred to the irradiance on the sample. While BTDF measurements have been widely carried out, a standard definition for this measurand does not currently exist. BTDF measurements are of interest for diverse applications ranging from diffusers for aero-space applications, for green-houses, luminaires and to functional glasses for photovoltaic panels, because they could allow better performance, characterisation and efficiency. Thus, the measurand of BTDF must be studied, primary facilities must be set up and traceability must be consolidated with sphere-based measurements.

Total appearance, as defined by the International Commission on Illumination (CIE), is the contribution of four main visual attributes: colour, gloss, texture and translucency. Currently, there is no metrology infrastructure in place for measuring translucency, even though this attribute is ubiquitous and crucial in many fields such as cosmetics, food, packaging, dermatology, architecture, virtual reality and 3D printing. Quantifying translucency requires traceable measurements of the Bidirectional Scattering Surface Reflectance Distribution Function (BSSRDF), which are not presently available.

3 Objectives

The overall goal of this project was to advance primary metrology in spectrophotometry. This involved defining the new quantities Bidirectional Transmittance Distribution Function (BTDF) and Bidirectional Surface Scattering Reflectance Distribution Function (BSSRDF), developing primary facilities for their realisation, and further improving the measurements of Bidirectional Reflectance Distribution Function (BRDF). The specific objectives of the project were:

1. To address advanced metrological issues, i.e. speckle and polarisation, related to measurement of the BRDF with the aim to reduce the measurement uncertainty by a factor of two, down to 0.1 % (k = 2) in the visible wavelength range,
2. To establish a full metrological traceability of the BRDF from very small objects (micrometre scale) to regular objects (centimetre scale),

3. To develop primary reference facilities and reference samples (artefacts) for the measurement and dissemination of the BTDF as a traceable quantity with a relative target uncertainty of 0.5 % (k = 2),
4. To develop primary reference facilities and reference samples (artefacts) for the measurement and dissemination of the BSSRDF as a traceable quantity with a relative target uncertainty of 5 % (k = 2),
5. To facilitate the uptake of the technology and measurement infrastructure developed in the project by the measurement supply chain (NMIs, spectrophotometer manufacturers), standardisation organisations (ISO, CIE) and end users (e.g. automotive industry, video game developers, healthcare sector, visual arts sector, architectural materials manufacturers).

4 Results

4.1 Advanced metrological issues related to measurement of the bidirectional reflectance distribution function (BRDF)

Over the last ten years, BRDF metrology has progressed considerably thanks to a European effort made by NMIs within the EMRP project IND52 xDReflect (2013 – 2016) and EMPIR project 16NRM07 BiRD (2017 2020). During these years, a first international comparisons of the BRDF scales have been done on the visible spectral range, for the geometries 0°/45° and 45°/0°. It was a first step. It pointed out also items that need to be explored in order to follow on progresses on BRDF measurement. First was the effect of polarization on the measurement. Second was the effect of coherence of light when increasing the angular or spectral resolution. And third what the control of directions of illumination and of observation. Additional details on background and discussion of the projects' results can be found in the published papers from the project listed in the section List of publications at the end of this document [1-15].

4.1.1 Effect of polarization on BRDF measurements

Polarization effects in diffuse reflection measurements at the transition between the UVA and VIS spectral range

Polarization effects play an important role in diffuse reflection measurements. Even for matte, quasi-Lambertian reflection samples, a large degree of polarization (DOP) can be induced by reflection in certain bidirectional geometries. To study this effect, the Stokes parameters of the reflected light have been determined for several samples at the transition between the visible (VIS) and ultraviolet (UVA) spectral range. As radiation source, a newly designed LED-based sphere radiator has been characterized and applied.

It was shown that the DOP increases with decreasing reflectivity at any specific wavelength in the VIS and UVA spectral range (Figure 1, Left). The DOP also depends on the bidirectional geometry, with larger values at larger incident or reflection angles (Figure 1, Right). Modelling of the angle-dependent spectral radiance factor confirms this observation [8].

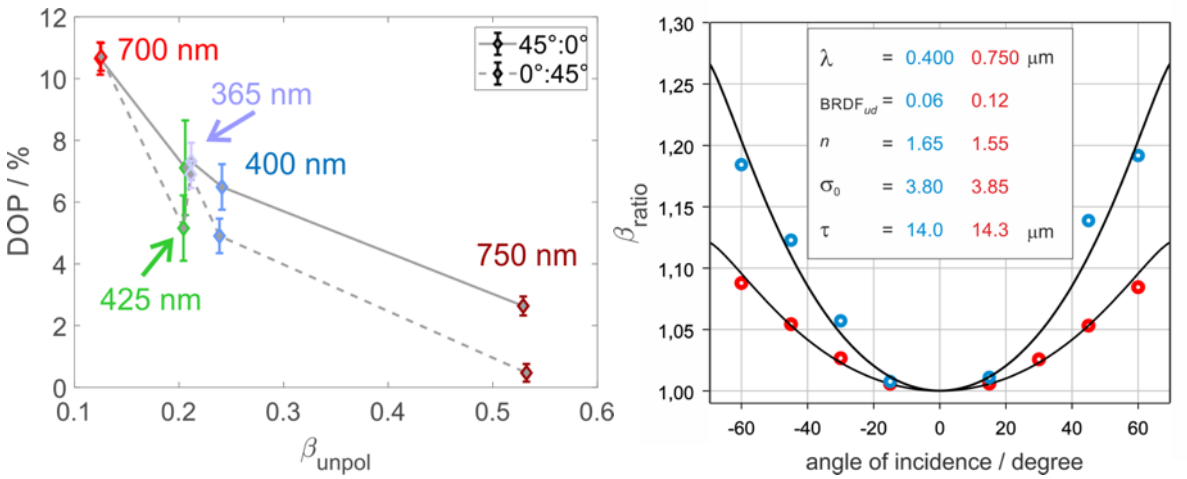

Figure 1: Left : Relation of DOP and reflectivity for different wavelengths. Right : Measured spectral radiance factor ratio and result of modelling for varying angle of incidence

Accounting for polarization–related effects in the measurement of the bidirectional reflectance distribution function

When measuring the BRDF to characterize typical materials, the effect of the polarization of the light source or the dependence of the detector on the polarization is not usually considered, even though many studies have proven their impact in the uncertainty of the BRDF of most materials, including diffuse reflectance standards. A methodology to assess polarization-related effects proposed by other authors has been tested by CSIC for the measurement of the BRDF of four typical materials used for realizing white diffuse reflectance standards (ceramic tile, barium sulfate, Spectralon and Russian opal glass). Relative systematic error due to polarizing conditions is calculated as a combination of the instrument polarization bias and sample-based coefficients, and the impact of the proposed methodology on the uncertainty was discussed.

Bidirectional radiance factors were measured at four linear polarization configurations pp, ps, sp and ss, and in different measurement geometries. A methodology for this kind of measurement has been proposed, which allows the relative systematic error due to the polarizing conditions to be estimated from sample-related coefficients and instrument degrees of polarization. The calculation of the sample-related coefficients (C1, C2 and C12) has been explained (Figure 2). Representative values for different kind of materials should be obtained and reported, in a similar way as done in this work for white diffuse materials. That would allow the uncertainty budget in the bidirectional reflectance measurements to be improved, and to recommend tolerances on polarization bias for commercial instruments, as a function of the kind of material intended to be measured. Finally, the impact of the proposed methodology on the uncertainty has been discussed [2].

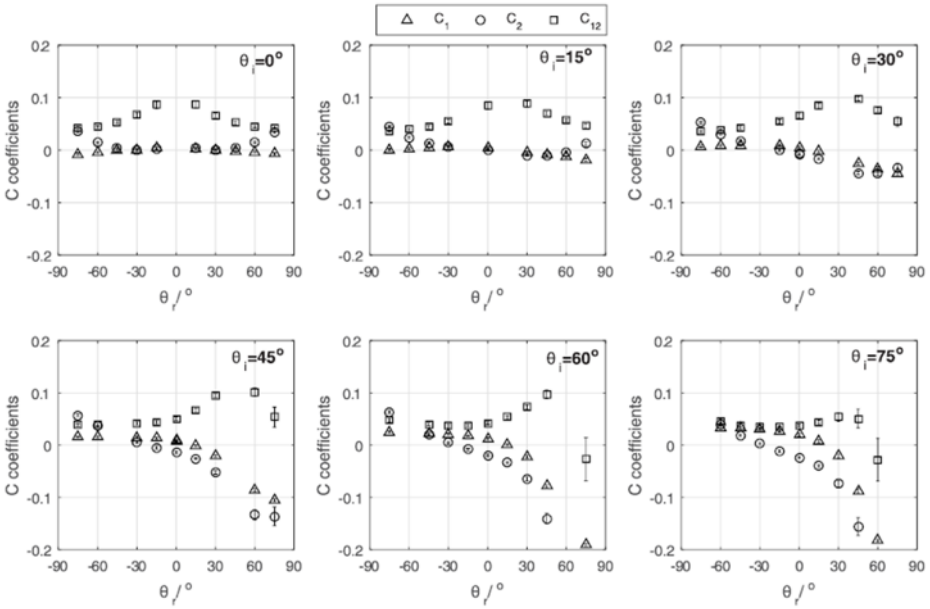

Figure 2 : Calculated spectrally-averaged C1, C2 and C12 coefficients for a diffuse reflectance standard ceramic tile.

4.1.2 Effect of coherence of light in BRDF measurements

Several visual effects are based on very steep radiance variation according to the direction of observation. It is the case for instance of high gloss surfaces, or of sparkle effects. In order to better characterize these effects, the community is developing goniospectrophotometers with high angular resolution. This equipment often uses incoherent light sources and a spectral bandwidth of several nanometres. However, even under these conditions, the new devices can reach such high angular resolutions that interference effects appear in the measurements.

A full study has been done at CNAM in close collaboration with UJM to confirm that these interference effects are speckle, a phenomenon rarely observed in incoherent light. Then proposals of techniques to overcome, at least partially, the speckle "problems" in BRDF measurements in order to recover the signal of the surface as if it had been illuminated in totally incoherent light have been formulated.

Concretely, BRDF measurements were performed by CNAM at very high angular resolution (0.017°) on surfaces of three different roughness and using light beams of three different cross-sections and with three different spectral bandwidths.

Samples used for this study were realized on purpose by NCS. It is a gloss scale on glass substrate with 3 different levels of gloss in black and in white. RISE could provide the full microtopography of these sample with the resolution suitable with the angular resolution of CNAM's goniospectrophotometer.

The statistical parameters and interference patterns of the measurements were compared with the speckle theory. This first work allowed to rule out the hypothesis of simple "noise" in the measurements and to confirm that measurements at very high angular resolution show speckle.

A model was then developed at UJM to simulate the BRDF of a surface by integrating optical interference. This model takes the instrument specifications (wavelength, spectral bandwidth, illuminated surface area, solid angles of illumination and observation) and the three-dimensional topography of the surface, and simulates the BRDF of this surface. The study was carried out in the visible range, for surfaces illuminated by circular beams of a few millimetres in diameter and for an area of the hemisphere restricted to a cone of ±1° around the specular direction. The surfaces studied were glossy and therefore of low roughness. The result of the simulations is in agreement with the measurements (Figure 3) [7].

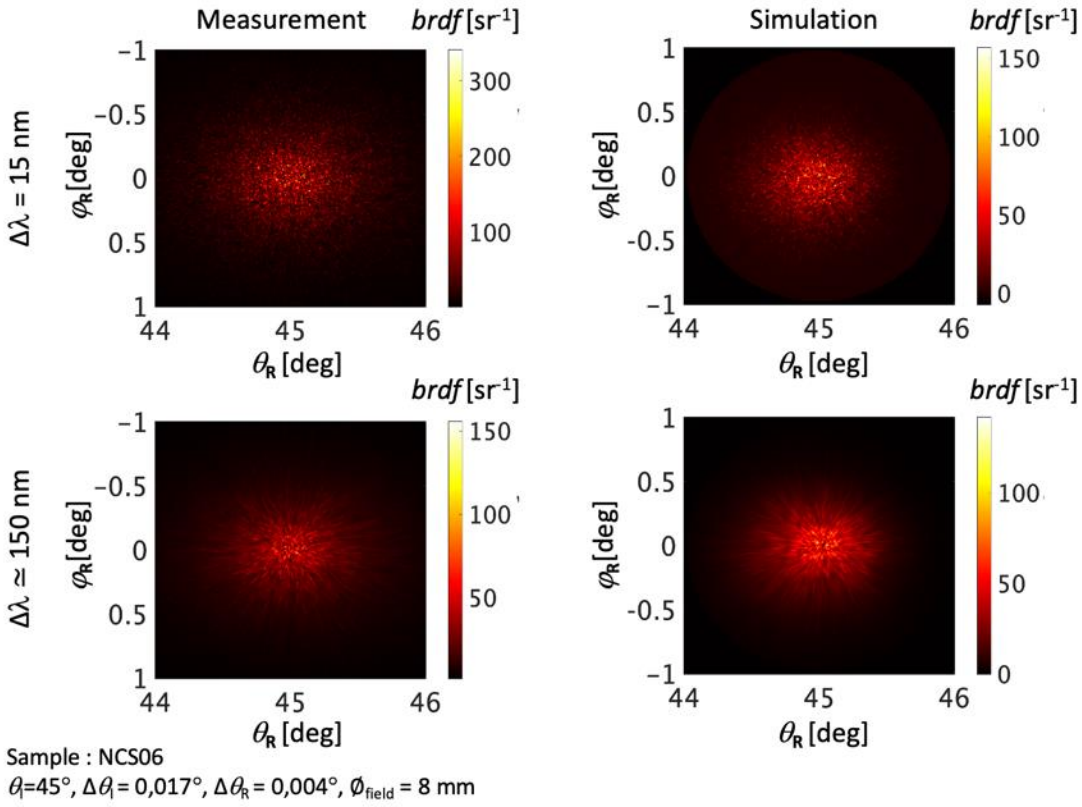

Figure 3 : Measurements (left) and simulations (right) of the bidirectional reflectance around the specular direction for a glossy sample with a Δl = 15 nm (up) and $\Delta l \simeq$ 150 nm (low) spectral bandwidth. Even if the light source is non-coherent, a speckle partially developed can be seen on the measurement because of the very high angular resolution of the device (0,017°). When the spectral bandwidth increases, the speckle shows a radial pattern more and more visible. The optical study allowed to model this effect that had never been clearly identified so far. These works allow to better understand the optical properties of materials.

4.1.3 Control of directions of illumination and of observation

CI studied the alignment errors of instruments with multiple rotation axes, such as goniospectrophotometers. These alignment errors contribute to the total uncertainty in the measured values of quantities such as the BRDF and BTDF. Even quite small uncertainties in the rotation and alignment of rotation stages can accumulate and propagate through the measurements to have significant contributions in the final uncertainty budget. To fully understand the effects of these errors on the measured values, a measurement model that explicitly relates the measured value to the physical sources of error in the rotation stages is required.

At CI, a detailed measurement model has been developed that considers errors in the displacement and angular offsets of the rotation axes along with errors in the accuracy, resolution, and zero offsets in the angles set by the rotation stages. The GTC Python package was used to input and track the uncertainties through the measurement equations of the model so that the contribution of each error could be identified in the uncertainty budget of the measured value.

The construction of the measurement model allowed CI to improve its uncertainties in BRDF through a better understanding of the goniospectrophotometer. By looking at the effects of each input error, the poses and measurement schemes could be chosen to optimise the uncertainty achieved. For example, Figure 4 shows the standard uncertainties in θ_i as θ_d and ϕ_d vary over the hemisphere. (Note that to achieve any given θ_d, ϕ_d geometry, all four rotation stages in the CI goniospectrophotometer may need to be rotated). In this example it was found that the largest uncertainties are incurred when the angle of the 'roll' rotation stage is large. Since in this case there are two choices of pose for the system to achieve a given geometry, a pose can be chosen to minimise the angle on the 'roll' rotation stage and move other stages instead. Figure 4 shows that by setting the instrument into the pose with the roll angle minimised, a smaller uncertainty is obtained. In another example, it was found that by taking advantage of negative correlations between measurements in different poses, the standard uncertainty in integrated diffuse reflectance could be reduced from 0.0029 to 0.0015 without additional measurement time [11].

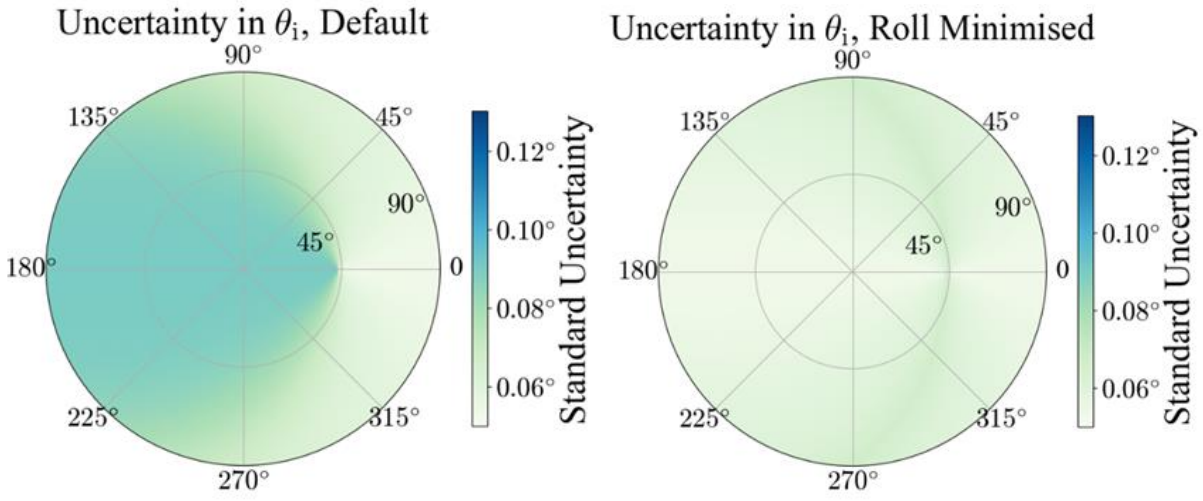

Figure 4 : Standard uncertainties in θ_i with fixed incidence angles $\theta_i = 45°$ and $\phi_i = 0°$ as θ_d and ϕ_d vary over the hemisphere. In the left image, the default pose of the instrument has been used, whereas in the right image, the pose that minimises the roll angle has been selected, decreasing the uncertainty in θ_i for much of the hemisphere.

4.1.4 Intercomparison of BRDF scale at in- and out-of-plane geometries

A multilateral scale comparison of BRDF measurements has been performed between METAS, CSIC, CI, LNE-CNAM, PTB and CMI. Each participant measured three achromatic samples in five measurement geometries: three in-plane and two out-of-plane geometries (Table 1). The geometries are defined in terms of spherical coordinates as $((\theta_i, \varphi_i):(\theta_r, \varphi_r))$, where θ_i is the incidence polar angle, φ_i the incidence azimuthal angle, θ_r the reflection polar angle, and φ_r the reflection azimuthal angle, all expressed in degrees.

Table 1. Measurement geometries used in the comparison

	Geometries
in-plane	(45°, 0°) : (0°, 0°) (0°, 0°) : (45°, 180°) (45°, 0°) : (60°, 180°)
out-of-plane	(45°, 0°) : (45°, 90°) (45°, 0°) : (50.1°, 146.6°)

The measurement comparison included two nominally identical sample sets (#1 and #2), which consist of three achromatic samples: two sintered Polytetrafluoroethylene (PTFE) samples and one satin sample. The two PTFE samples, provided by Labsphere, have nominal reflectance values of 99% and 50%. They were identified as PTFE99 and PTFE50. The satin sample was produced specifically for the measurement comparison by NCS. The sample consists of white acrylic paint spread by pulverization on a glass substrate to provide good support and ensure the sample's flatness and stability. In contrast to the two PTFE samples, the satin sample is not a quasi-Lambertian sample: it has a nominal gloss value of 20 GU at 60° measurement geometry. The satin sample was identified as Satin20.

The measurand for the comparison was the BRDF of a 10 mm diameter area in the centre of each sample in the above defined five geometries for unpolarized light of 550 nm with a 5 nm bandwidth. The parameters were carefully selected in order to avoid any polarization bias or speckle influence. Figure 5 depicts the measured BRDF values along with the reported expanded uncertainties.

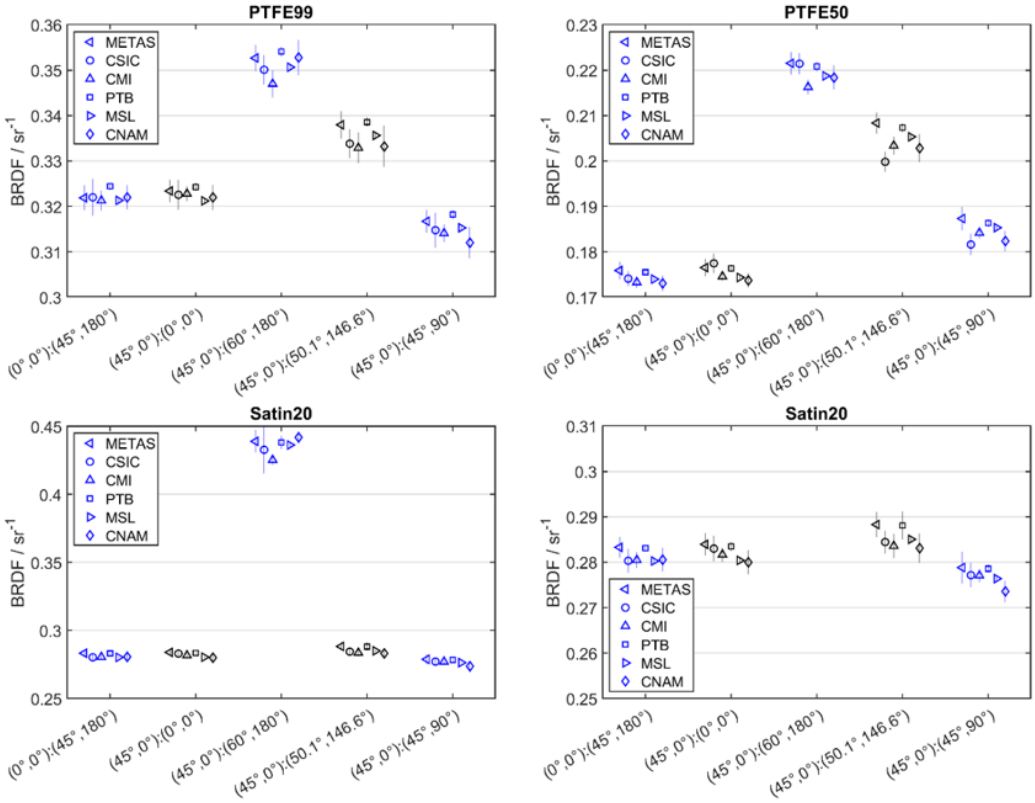

Figure 5: Measured BRDF values (markers) along with the reported expanded () uncertainties (bars). The Satin20 sample is represented in two different scales in order to better show the values at all measurement geometries.

The reference value was computed using the Mandel-Paule method, where an interlaboratory uncertainty component is added to all participants' uncertainties until the data passes the Chi-square test. The iterative process was executed for every sample and every geometry separately. The results demonstrated some discrepancies between the measurement scales. A non-negligible contribution of interlaboratory uncertainty was estimated to achieve consistency. The most probable cause for the discrepancies is the underestimation of the uncertainty contributions [12].

4.1.5 Recommendation of samples

Based on the outcome of the BRDF comparison (see § 4.1.4), it can be concluded that the selected samples are suitable for the highest realization of BRDF. The consortium recommends using three samples to test goniospectrophotometers traceability :

- A sintered Polytetrafluoroethylene (PTFE) sample with nominal reflectance values of 99 % can be considered as the “easy” sample. It allows to test the facility at its best performance to get the level of its best uncertainty reachable.
- A sintered Polytetrafluoroethylene (PTFE) sample with nominal reflectance value of 50 % (or 10 %) can be used to test the signal to noise ration of the facility and its sensitivity to straylight.
- A satin white sample with a nominal gloss value of 20 GU at 60° measurement geometry can be used to test angular resolution of the facility as well as its sensitivity to misalignment. The sample developed by NCS, consisting of white acrylic paint spread by pulverization on a glass substrate to provide good support and ensure the sample's flatness and stability was well appropriated.

The topography of the samples, measured by DFM using a Zygo NX2 optical profilometer, is shown in Figure 6. It provides orders of magnitude of roughness and flatness required to get satisfying results.

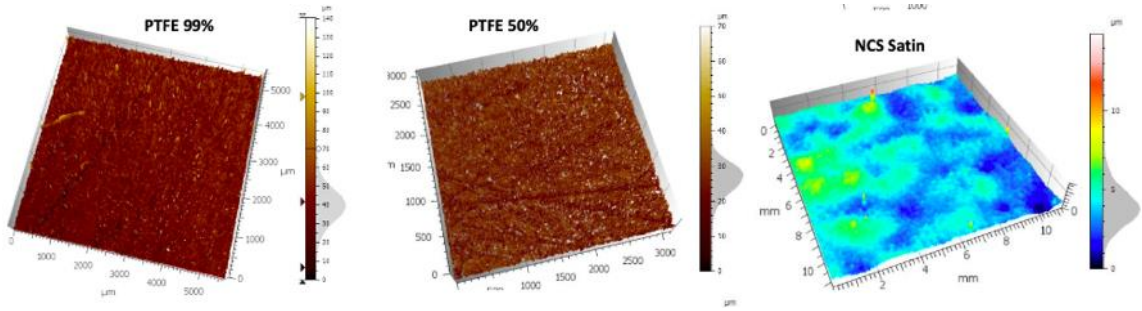

Figure 6 : Surface topography for the sample types recommended for BRDF comparison

Although the exact samples used in the comparison may not be directly commercially available, the two PTFE samples are similar to the Spectralon® material available from Labsphere commonly used as reference standards for BRDF. However, other kind of PTFE based materials may be equally well suited in that respect.

4.1.6 BRDF models

For modelling relatively large random surface roughness, a method called Generalised Harvey-Shack (GHS) has been developed by Krywonos et al.. GHS is a transfer function describing the interaction between light

and a rough surface, provided that the surface Power Spectral Density, PSD (or alternatively the auto-correlation function, ACF) is known, and that the surface has a Gaussian height distribution. Then

$$f_r(\theta_i,\phi_i;\theta_o,\phi_o) = Q\,\mathcal{F}(H_s(\hat{x};\mu_i,\mu_o))$$
$$H_s(\hat{x};\mu_i,\mu_s) = \exp\left[-(2\pi\hat{R}_{q,\mathrm{rel}}(\mu_i+\mu_s))^2\left(1-\frac{\mathrm{ACF}(\hat{x})}{R_{q,\mathrm{tot}}^2}\right)\right],$$

where F is the Fourier transform, $\hat{x} = \frac{x}{\lambda}$, $\mu_i = \cos\theta_i$, $\mu_o = \cos\theta_o$, $\hat{R}_{q,rel} = \frac{R_{q,rel}}{\lambda}$ is the band limited RMS roughness found by integrating the PSD curve over the frequency interval 1/d < n < 1/l. Here, d is the diameter of the measurement spot, 1/l is the spatial frequency limit for propagation modes and $R_{q,tot}$ is the total RMS roughness found by integrating the experimental PSD curve over the entire positive frequency range $1/d < n < 1/\lambda_{cut}$, where $n_{min} = 1/d$ and $n_{max} = 1/\lambda_{cut}$ are the experimental cutoff frequencies of the instrument. Consequently,

$$R_q^2 = 4\int_{\nu_{min}}^{\nu_{max}} \mathrm{PSD}(\nu)\,d\nu$$
$$R_{dq}^2 = 4\int_{\nu_{min}}^{\nu_{max}} (2\pi\nu)^2\,\mathrm{PSD}(\nu)\,d\nu\,.$$

The two-dimensional PSD from a physical surface may be obtained from microscope images of a surface and turned into the one-dimensional PSD considered here by image averaging along the sample BRDF measurement direction. It is advisable to use a PSD curve with a wider frequency range than the frequency range obtained by transforming the BRDF angles into frequency space. This can be achieved by making confocal microscope images of the same area with different numerical apertures and plotting them together as one PSD plot. The PSD plot is then fitted using the ABC model (the K-correlation model) over the entire frequency space. The ACF may be obtained as the inverse Fourier transform of the PSD curve and the roughness parameters by integrating the PSD curve in the equations for R_q and R_{dq} above.

It is very important to realize that the presented PSD formalism enables us to link the nano/micro length scale with the macroscopic mm/cm length scale. The PSD method thus provides a uniform, scale-independent method for scattering estimation. Here, we show the results for the ABC model with $C = 2$, which is typically a good approximation:

$$\mathrm{PSD}_k(\nu) = \frac{A}{1+(B\nu)^2}$$
$$\mathrm{ACF}(\hat{x}) = \frac{\pi A}{B}e^{-\frac{2\pi\hat{x}}{B}}$$
$$R_q^2 = \frac{4A}{B}\arctan(Bf)\Big|_{f=\nu_{min}}^{f=\nu_{max}}$$
$$R_{dq}^2 = \frac{16\pi^2 A}{B^3}(Bf-\arctan(Bf))\Big|_{f=\nu_{min}}^{f=\nu_{max}}.$$

The use of the ABC model enables us to perform the inverse Fourier transformation and the integration analytically, which is a great help in fitting the GHS to an observed BRDF and thereby obtaining the resolution-limited surface information from the data. The improved GHS theory developed by DFM in this project was detailed in a published article [10].

4.1.7 General consideration of BRDF

From an optical point of view, the current definition of BRDF is incomplete. This quantity implicitly assumes spatially incoherent light, which prevents any interference. It also assumes that the limit of illumination of the surface from one single direction, therefore by a plane wave with a zero solid angle, can be reached. But that is precisely the case of maximal spatial coherence, prone to interferences that will occur after scattering by the sample. Similarly, geometrical optics is assumed valid on the light collection side, ignoring diffraction by the sample. But a minimal collection solid angle corresponds to the most visible diffraction effects, which are however intrinsic to the phenomenon of scattering by small random fluctuations in the surface roughness and manifest themselves as speckle. Therefore, speckle effects are ignored by that definition, while they are in fact maximized in the limit of the narrowest possible solid angles on the illumination and/or collection side.

Actually, until recently, the question of coherence was not an issue for BRDF measurement since most devices had a solid angle ω_i large enough that coherence effects were not observable. Similarly, the rather large collection solid angle ω_o did not allow to resolve any speckle pattern, but instead averaged the radiance and blurred speckle grains. However, recently, high-resolution BRDF measurement devices have considerably increased the directionality of the incident beam as well as the achievable angular resolution at collection. Consequently, speckle is clearly visible in the measurements (Figure 7).

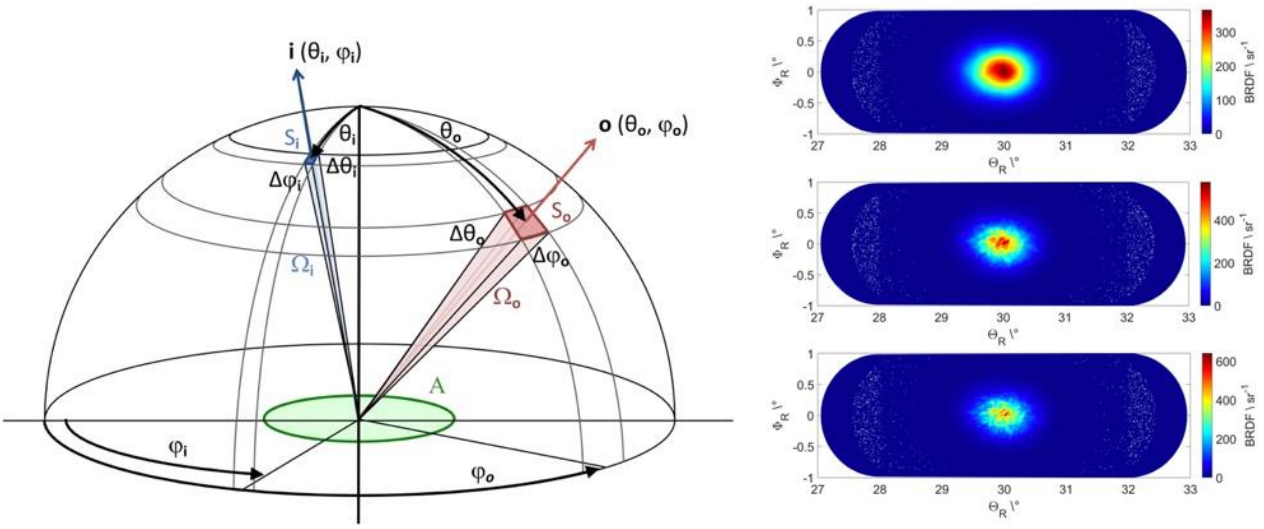

Figure 7 : Left : notations used for BRDF definition. Right : BRDF of a high gloss black sample extracted from NCS gloss scale ($gloss_{60°}$ = 95 GU) around the specular direction. Illumination θ_i = 30°, ϕ_i = 180°, V(λ) spectral range. Angular resolution is 0.315° (top), 0.057° (middle), 0.029° (bottom). Speckle appears when resolution decreases.

Notice in addition that speckle patterns depend on wavelength of light. The most contrasted patterns are observed with monochromatic radiations. In case of white light or broad spectral bands, the speckle patterns produced by each wavelength add to each other on an incoherent basis. If the detection is not spectrally resolved, the contrast of the speckle patterns decreases or may even disappear, at least far from the specular direction. In the case of very high angular resolution, however, even though the incident light has V(λ) spectrum, the observed speckle has a rather high contrast due to the small solid angles (Figure 7, right).

Enforcing a definition for BRDF that assumes incident light source to be perfectly spatially incoherent, i.e., in which coherence of light is not a parameter would entail considering that speckle is not part of the measured BRDF but rather an experimental error, even though, in certain conditions, this error cannot be removed. To be convinced of this, one may consider a perfectly homogeneous scattering material with uniform appearance: Its BRDF should by definition be the same since the microstructure responsible for scattering is statistically uniform, whereas the speckle patterns varies strongly from one area to another due to the variations of local microstructure.

Based on these considerations, UJM and CNAM propose a new definition for BRDF representative of the scattering properties of the material "as if" the incident beam was spatially incoherent. Following earlier work by Hoover and Gamiz, they suggest that this can be achieved by considering, at each wavelength λ and for given polarization states on both sides, the expected value of the radiance scattered by the sample over areas whose random structure is statistically similar but independent from each other. In practice, over areas which do not overlap with each other, we have:

$$f(\mathbf{i},\mathbf{o}) = \frac{\langle L(\mathbf{i},\mathbf{o})\rangle}{E(\mathbf{i})}$$

where f is the BRDF, L is the radiance in the direction **o** and E is the irradiance from direction **i**.

The BRDF measurement in each area includes a random fluctuation due to speckle, but the average of all measurements will discard these fluctuations whose expectation is zero. The number of measurements to be averaged depends on the solid angle of illumination: as a smaller solid angle induces a more contrasted speckle, the number of measured areas must be increased, which requires a larger sample. The manufacturers of measuring devices should explicitly state the way to obtain the mathematical expectation of the radiance according to the device's characteristics. If the incident solid angle is large enough to be considered as

incoherent, one radiance measurement suffices. The new BRDF definition is then equivalent to the usual one. The user must just be aware of the limitation in terms of angular resolution. Having these results, the project successfully achieved the objective [9].

4.2 Establishment of a full metrological traceability of the BRDF from very small objects (micrometre scale) to regular objects (centimetre-scale)

As a consequence of the development of virtual prototyping, 3D printers and micromachining, a need of BRDF measurements made on micrometric surfaces has shown up. But so far, national standard of BRDF are developed only on centimetric surfaces. And effort has been made in the project to develop goniospectrophotometers capable to do measurements on tiny surfaces. Once this step done, the consortium has worked on the extension of the BRDF traceability from centimetric scale to micrometric scale.

4.2.1 Samples for µBRDF measurement

A large selection of both custom-made as well as commercially available samples was used for the BRDF measurements of small size samples and multi-scale traceability. An overview of the samples is presented in Figure 8. In addition, two types of micropillar structured glass samples and five different types of glass fibre samples have been supplied by SG, and a Spectralon® diffuse reflectance standard was used. Various issues were encountered when the samples were evaluated, such as translucency of the Spectralon® sample at small beam sizes and non-homogenous or curved surfaces when the beam size is reduced (fake leather, glass fiber sheet, nylon threads). The results are reported elsewhere but the conclusion is that none of the samples are suitable as standard artefacts, and that further work is required related to small size BRDF measurements and multiscale traceability.

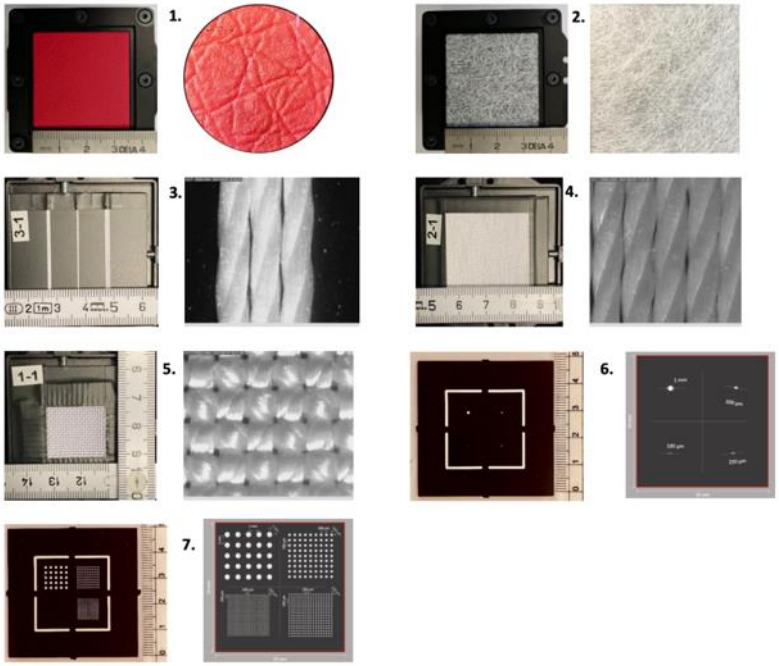

Figure 8: Left Samples for small size BRDF measurements and multiscale traceability: 1. Red fake leather, 2. Glass fiber sheet, 3. Nylon thread samples (1, 2 or 3 threads), 4. Nylon thread sample (parallel threads), 5. Woven nylon thread sample, 6. Sample with 4 white dots diameter 1 mm, 500 µm, 300 µm, and 100 µm, 7. Sample with three white dots grids, dot diameters 1 mm, 500 µm, and 300 µm.

4.2.2 Development of µBRDF measurement facilities

At DFM

The micro-BRDF setup employed by DFM is shown in Figure 9: A diode laser (Oxxius LBX-660-100-CIR-PP) running at a wavelength of 663 nm illuminates a spot on the sample. A focusing lens is employed to control the size of the measurement spot, which can reach mm scale diameters. The measurement is performed in

an underfilled configuration, meaning that the measurement area is limited by the illumination area, which is smaller than the acquisition are of the detector. A Si detector (New Focus 2032) mounted on a rotary arm scans the reflection angles in the horizontal plane. In order to improve the angular resolution of the measurement, a 200 mm wide slit was placed in front of the detector.

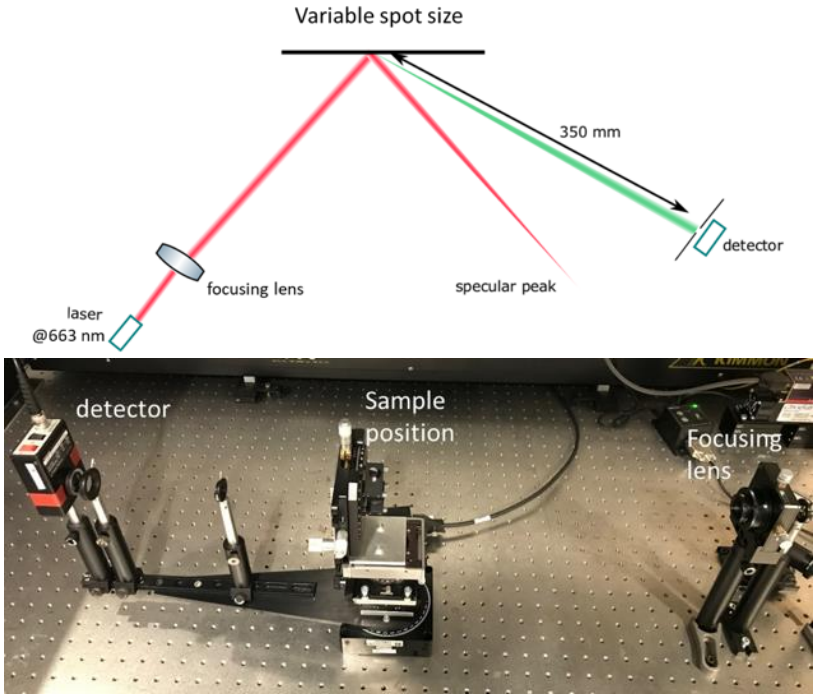

Figure 9: (top): Schematic of the goniometer employed by DFM for BRDF measurements with varying spot sizes. A focusing lens is used to generate illumination spots of varying size. *(bottom) Photo of the BRDF measurement setup.*

At CNAM

CNAM developed a new measurement line dedicated to the measurement of the "micro" Bidirectional Reflectance Distribution Function (µBRDF), meaning an absolute measurement of the BRDF at a submillimeter scale. The experimental setup has been designed to measure the BRDF with spectral information within the visible spectrum, for any direction of the hemisphere, on a circular area of diameter inferior to 100 µm, and with an angular resolution inferior to 2°.

The µBRDF gonio, shown in Figure 10 (left), comprises an illumination system, a detection system, and a 6-axis robot arm as sample holder. The µBRDF is measured in an underfilled configuration, that-is-to-say, the illuminated area is included in the measurement area. The sample is held on a 6-axis robot arm (RV 12S, Mitsubishi) and positioned at the center of the gonio using the robot translation and orientation features. The illumination system is placed on a breadboard that can rotate around the sample in the room horizontal plane using a rotation ring to measure the µBRDF at any geometry of measurement, i.e., any angle of the hemisphere for the illumination and observation directions. The center of the gonio, which also defines the position of the sample plane, corresponds to the center of the ring.

The illumination system comprises a Laser Driven Light Source (LDLS – EQ99, Hamamatsu), chosen for its high power, good stability and spectral emission that covers well the visible range. An optical system has been designed to image the source plasma at the center of the gonio with a magnitude of 0.1 in theory. In practice, the light beam on the sample plane has a gaussian power profile with a full width at half maximum of roughly 30 µm, and the illumination beam is converging with an aperture that can be adjusted using an iris diaphragm to an angle up to 1.5°.

The detection system is a CS2000 spectroradiometer (Konika Minolta), chosen for its good spectral resolution (1 nm) and for its ability to measure small levels of radiance. However, the CS2000 entrance optics is not well adapted to measuring on very small areas and does not have a sufficiently large aperture. Consequently, CNAM removed this optics and replaced it by an optical system designed to measure within a field of view of 0.01° rather than the original 0.1°, which corresponds to an area of roughly 300 µm on the sample plane in (Figure 10, right), with an entrance pupil large enough to measure incident beams of aperture up to 1.5°.

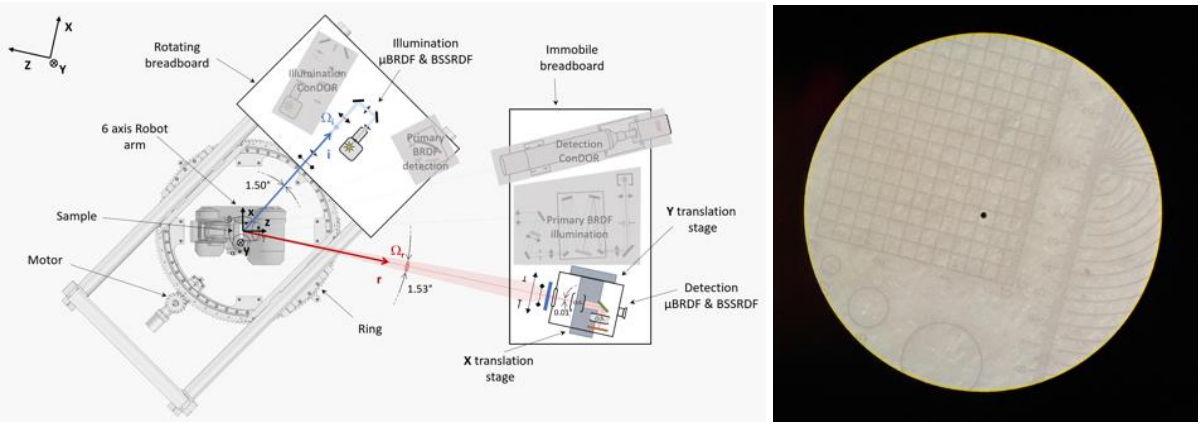

Figure 10: Left : Schematic representation of CNAM goniospectrophotometer facility showing the mechanical elements, the detection and the illumination units used for primary µBRDF measurements. The shaded elements are used for the other types of measurements on the same facility. Right : The black dot is the field of the detection system, with a diameter of 300 µm

To validate the µBRDF gonio, a classical approach based on comparing BRDF measurements carried out on a white diffusing calibration standard measured at both micrometric and centimetric scale is not possible, because the reflectance properties of the standards aren't invariant to scale variations at such small scales, due to their surface roughness and the translucency of their material. CNAM identified this issue through the measurement of the µBRDF on two types of samples, a white diffuser (Spectralon) and a NCS gloss sample (white coating on glass). To overcome this issue, CNAM fabricated samples designed to limit the issues linked to translucency, made of black plexiglass onto which holes of sizes ranging from 100 µm to 1 mm were drilled, then filled with white resin and sanded to obtain a diffusing surface that presents white disks on a black background.

At METAS

The µBRDF setup at METAS is shown in Figure 11. It performs relative measurements using a reference sample with traceability to PTB. The illumination is quasi-monochromatic using a commercially available tuneable light source with a wavelength range of 390 nm up to 700 nm. A Köhler optical system ensures that the sample is illuminated uniformly with a quasi-collimated beam. The beam size of the illumination was adjusted by changing the aperture 1 (see Figure 5), ranging from 200 µm up to 20 mm in diameter. The detector is a CCD camera with an integrated filter wheel, which can be used to directly measure the chromaticity coordinates when used together with a broadband light source (LDLS) instead of a tuneable one. The measurements were performed either by changing the beam size and averaging over a larger measurement area, or by keeping the beam size large and selecting only a smaller measurement area.

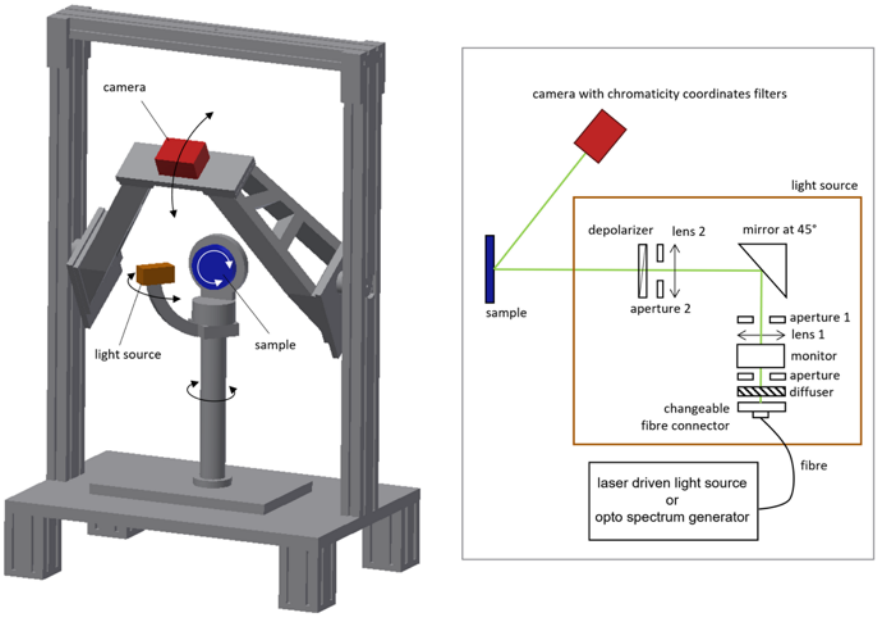

Figure 11: Schematic representation of METAS goniospectrophotometer facility showing the mechanical elements, the detection and the illumination units used for μBRDF measurements.

At CSIC

The measurements have been carried out with our goniospectrophotometer, GEFE, which has been improved by including a high sensitivity CMOS digital camera as a new detection system and a laser driven light source which, together with an optimization of the optical irradiation system, provide us a higher irradiance on the sample plane. For multiscale measurements, CSIC has used a uniform irradiance in an area of 2 mm length or an optical configuration in which a pinhole wheel was used. This pinhole wheel, with 16 different hole sizes from 25 μm to 2 mm in diameter, was put on an image plane of the light source with the aim of obtaining an image of the selected pinhole on the sample plane, thus reproducing different small irradiation areas. In Figure 12, the experimental setup used in each case with its respective rim rays diagram is represented. Having these results, the project successfully achieved the objective.

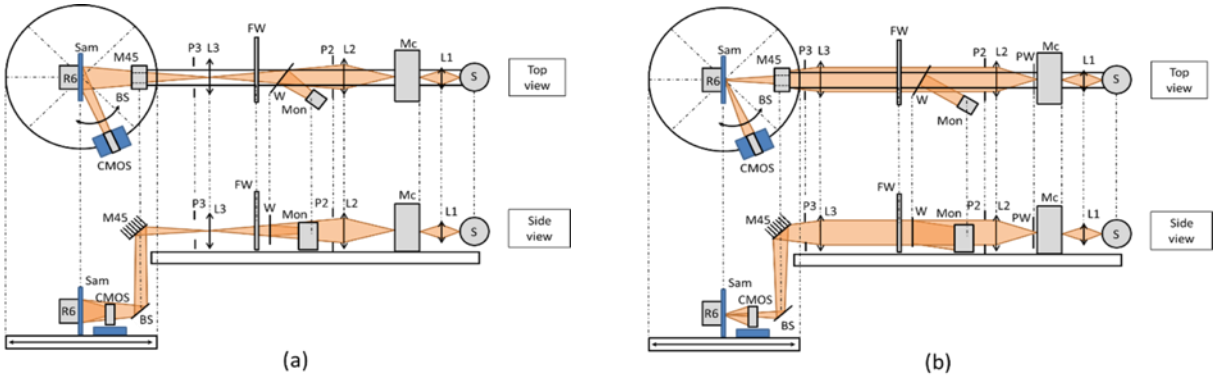

Figure 12: Configuration of the irradiation optical system for the measurements of (a) Activity 1.4.2 and (b) Activity 1.5.1.

4.3 Development of primary reference facilities and reference samples (artefacts) for the measurement and dissemination of the bidirectional transmittance distribution function (BTDF) as a traceable quantity

BTDF as a quantity is the angle dependent radiance in transmission, referred to the irradiance on the sample. Although most of the high precision goniospectrophotometers developed at NMIs for BRDF measurement can also perform BTDF measurement, no CMC entry exists for BTDF measurement and no congruent international

scale can be guaranteed. But there is a growing need of BTDF measurement for quality control of diffusers used in LED luminaires, greenhouses or for specific directional functionalities.

The project addressed this technical topic by setting up 2 independent realisations of the quantity and by organizing a BTDF comparison to test the traceability.

4.3.1 Selection of appropriate samples

During the project, two comparisons on BTDF were carried out. In total, seven types of samples were included in the comparisons consisting of a mix of commercially available samples and samples developed specifically for project by Innventia.

The samples can roughly be categorized as follows:

- **Category 1 : Quasi-Lambertian, bulk scattering**
  These samples exhibit a homogenous bulk scatter effect. The nominal scatter performance is independent with respect to azimuthal orientation and no polarization-dependence can be expected. Also, the variation of the BTDF with the scattering angle is low.
- **Category 2 : Dedicated scatter angle-dependence without azimuthal effect**
  These samples show peak function-like BTDF distributions, the less scattering ones being close to Gaussian distributions. Compared with Category 1-samples, the BTDF values are higher by one to two magnitudes, but they also show no azimuthal dependence. This type of transmittance can be achieved by surface scattering (case of ground-glass diffuser) or by bulk scattering (case of transparent resina with scatter pigments)
- **Category 3 : Dedicated scatter angle-dependence with pronounced azimuthal effect**
  For this category two sample-types were chosen which possess a special microstructure as active surface. The active elements have a thickness of less than a millimetre and are carried by non-scattering bulk material. One sample consists of a specially formed micro-lens structure resulting in an angular scatter distribution with a square dependence. Inside the square, characterized by a nominal edge angle, the BTDF is roughly constant, experiencing then a sudden drop to almost vanishing scatter for angles larger than the edge-angle. One sample behaviour is based on holographic technique, resulting in an elliptical Gaussian-like scatter-distribution for two major axes, exhibiting different widths for the two perpendicular azimuthal orientations.

For additional information about the sample properties and the measurements carried out, see [14]. Note that the choice of commercial products does not constitute an endorsement by the BxDiff consortium, and other commercial products may provide equivalent results.

In Figure 13, typical experimental BTDF distributions are plotted for different sample types used in our comparisons. From the curves it is obvious that different experimental requirements must be fulfilled by a measurement device used to characterize the samples.

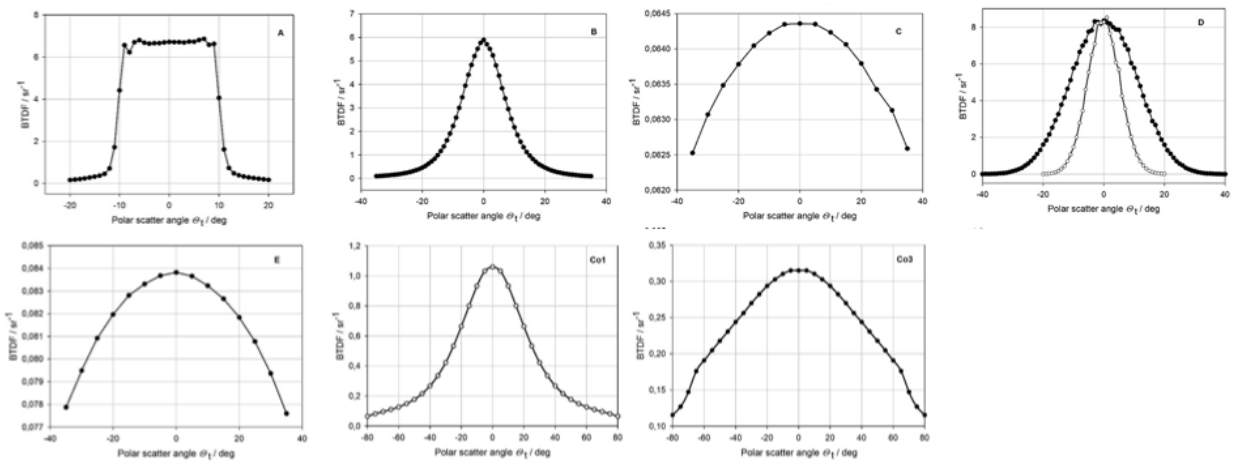

Figure 13: BTDF distribution measured in standard geometry (θ_i = 0°, ϕ_i = 0° and ϕ_d = 0° with varying θ_t). Micro lens structure (cat 3) giving a square shape BRDF (A), surface scattering (cat 2) giving a sharp gaussian BTDF (B), Quasi lambertian (cat 1) giving a large but low BRDF (C) & (E), Holographic structure (cat 3) giving elliptical BTDF (D), bulk scattering type giving a sharp gaussian BTDF (CoV1) & (CoV3)

Measurands of standard artefacts in the best scenario should not depend on experimental parameters like scatter angle, wavelength, beam size, etc. Also, a good temporal stability is required in which also some insensitivity against contamination should be contained. If two sample types should be chosen from the shown examples, one with less scatter angle dependence and one with some dedicated angle characteristics, no choice is ideal with respect to all requirements.

From the Lambertian-type samples one would concede that sample type C (Heraeus HOD®-500) is the most promising, as its Quartz material implies a good stability, and the wavelength-dependence is lower than for example compared with sample type E (Sphere Optics Zenith Polymer®). However, in view of the observed lateral diffusion issue, the preference would be given to E although this foil type sample needs special precautions for mounting it in a flat state. Also, the observed inter-sample variation for the E-type (~2,5 %) is smaller than that for the C-type (~6 %).

The azimuthal independent sample B (Thorlabs DG20-220) is a good choice for a sample with dedicated polar angle dependence. The fairly homogenous surface and a thin active surface makes it a good candidate. A possible further option is the bulk scatter sample type Co1 (Covestro IOL 1113-2 1mm, thin) which raises only small thickness issues and has a medium BTDF-value. However, as of now, this sample is not commercially available.

4.3.2 Independent realization of the BTDF measurement at PTB and Aalto

To determine the bidirectional transmittance distribution function (BTDF) of diffusely transmitting materials, two new primary facilities have been independently developed at PTB (Figure 144) and Aalto University. The performance of both facilities is compared by a bilateral comparison on two different diffuser types, one with a Lambertian, the other with a Gaussian scattering characteristic. The BTDF is determined in both in-plane and out-of-plane bidirectional geometries at four different wavelengths in the visible spectral range. A thorough analysis of the measurement uncertainty shows a combined k = 1 standard uncertainty of 0.8 % - 1.2 % (PTB) and 1.3 % - 1.7 % (Aalto). The BTDF results obtained agree well within their expanded k = 2 uncertainty, indicating that both facilities are suited as primary reference setups for the determination of the BTDF. Moreover, main contributions to the uncertainty budget have been identified and will be considered in future improvement of the systems.

At Aalto

The primary reference facility in Aalto University for BTDF measurements includes a 3D gonioreflectometer with traceability to SI. The instrument is calibrated by a reference material that is traceable to Aalto's absolute gonioreflectometer. The 3D gonioreflectometer has performed BRDF measurements of non-rigid samples, such as sand, using a horizontal sample holder. Furthermore, a thorough evaluation of the uncertainty budget in BRDF has been performed, which can be partly applied to BTDF measurements.

Figure 15 shows a digital render of the 3D gonioreflectometer in its configuration for BTDF measurements. The system includes an illumination part (1 and 2), a detection part (3 to 5), and sample holder (6). The illumination part includes an optical system with a monitor detector (1) that illuminates the sample by using a one-axis robot arm (2). Monochromatic illumination is produced by a combination of a super continuum laser and a laser line tuneable filter. The beam is transferred by fibre coupling to the optics system. The illumination is collected by the detection system, which includes a two-axis robot (3 and 4) that controls the viewing azimuth and zenith angles of the detector. The detector housing (5) collects the transmitted signal by using a 10 mm aperture and an off-axis mirror. The signal is directed to a set of two detectors, including a silicon, and an InGaAs detector, that cover a wavelength range from 400 nm to 1700 nm. The sample holder (6) allows for non-rigid samples, such as sand and liquids, of various sizes. Now, the transmitted signal can be measured in a half-sphere beneath the sample plane.

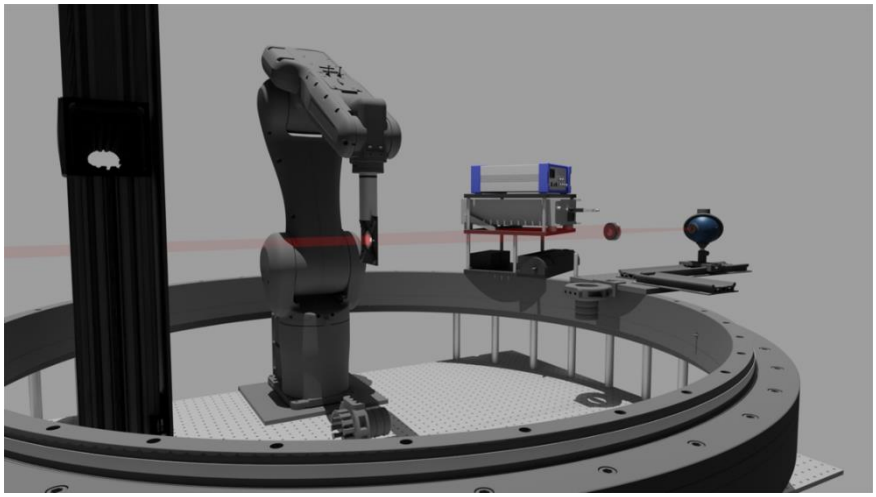

Figure 144: Sketch of PTB's new primary BTDF facility.

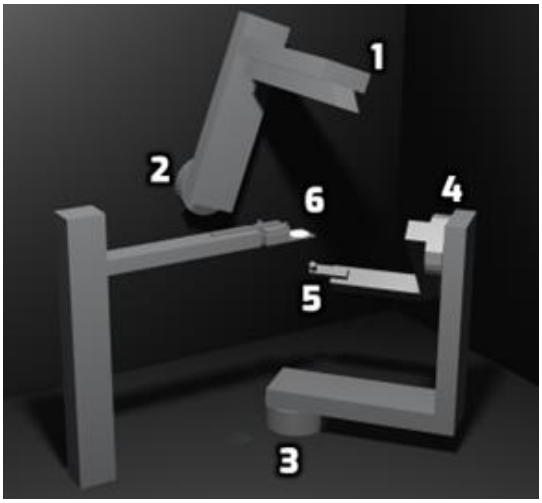

Figure 15: 3D render of the out-of-plane gonioreflectometer at Aalto

4.3.3 BTDF interlaboratory comparison

Two groups of multilateral scale comparisons on the measurand of diffuse transmission, the bidirectional transmittance distribution function (BTDF), were performed between National Metrology Institutes (NMIs), Designated Institutes (DIs) and industrial partners, to get an insight on existing European measurement capabilities and gain experience in the characterisation of a larger variety of different diffusers. In the first group of comparison, five NMIs and one DI have dealt with samples of three different scattering characteristics in different in-plane geometries, focusing more on orientation-dependent (azimuthal) scattering properties. In the second group of comparison, three home-built and three commercially available measurement setups were involved, with the emphasis lying on the scattering magnitude and sample thickness.

The measurement results were analysed and a first version for the peer-reviewed paper was issued to project partners for commenting. These comments are currently processed. Because of the enormous amount of results, the current length (> 25 pages), as well as the need to merge the results obtained from both groups, the completion of a ready for submission paper will take some more effort. However, it can be foreseen that the quality of the results will give an excellent overview of the European capabilities in performing high-class BTDF calibrations and will also show specific sample-related problems to be solved for improved future BTDF measurements.

4.3.4 BTDF modelling

The BTDFs of five types of transmissive diffusers were measured. For one of the samples, a holographic diffuser, an interesting phenomenon was observed in the interaction between angle- and wavelength-dependence of the spectral transmittance, see Figure 16. To explain this behaviour, we decided on a model based on separation of insurface and subsurface scattering. We used a single scattering model consisting of an active top surface with microfacets (insurface) and small scattering particles (subsurface) on a smooth transparent substrate. The microfacets obeyed a normal distribution determined by the surface roughness (standard deviation in height). The scattering by particles was based on Rayleigh scattering where the wavelength dependence was modified according to particle size. Even without considering multiple scattering, we observed a tendency in the simulated spectral transmittance similar to the one measured [4,14].

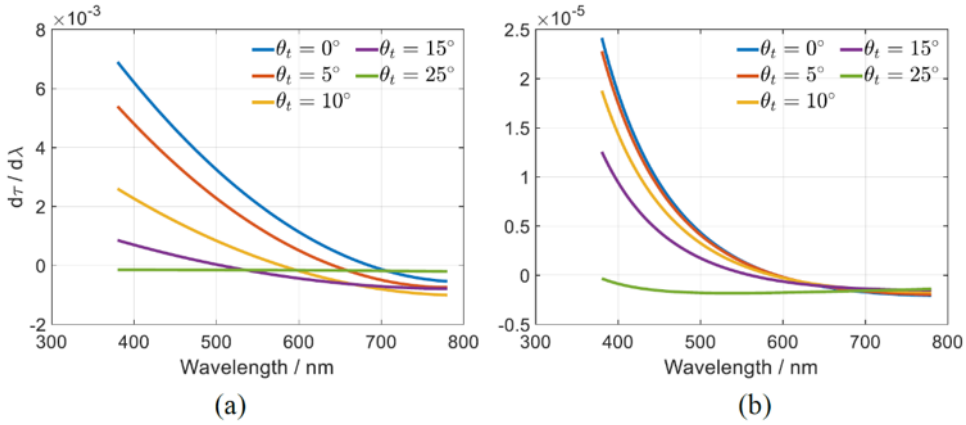

Figure 16. The derivative of transmittance with respect to wavelength. (a) A holographic surface sample, E28-14, illuminated at normal incidence and measured at different transmission angles θ_t. (b) simulation using a single scattering model.

4.3.5 Recommendation for BTDF measurement

The complete version of “Good practice guide for the measurement of BTDF” is published under https://bxdiff.cmi.cz/wp-content/uploads/2023/03/Good-practice-guide-BTDF.pdf on the webpage of the BxDiff project.

The measurement of BTDF (Bi-directional transmittance distribution function) can be regarded as the transmittance analogue of the BRDF (Bi-directional transmittance distribution function) determination and both are developed from general considerations on optical scattering by surfaces and solid bulk material. Therefore, all dependency on experimental parameters as well as uncertainty considerations can be transferred from the 'reflection' to the 'transmission' world. However, specific aspects should be taken into close consideration when performing accurate BTDF measurements.

The influence of the apparatus function is one important aspect. From calculation based on gaussian model scatter distributions with full width at half maximum ranging from 10° to 140°, the required resolution of the apparatus can be calculated as a function of a given deviation of the maximum value (geometry 0°, 0° / 0°, 180°). In Figure 17 the dependence between the spectrum's FWHM and that of the apparatus function can be read. For a given acceptable deviation, linear functions with varying slope are observed.

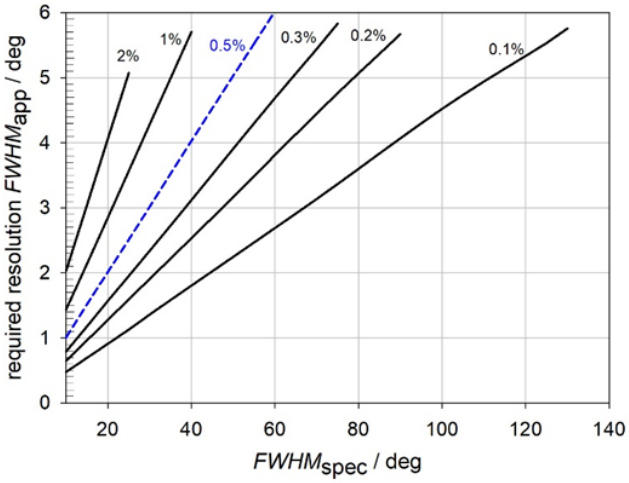

Figure 17 : Required resolution $FWHM_{app}$ of the apparatus needed to obtain a given maximum deviation for spectra with different angular broadness ($FWHM_{spec}$).

Another important aspect is the influence coming from sample thickness and enhanced lateral scatter. In measurements of the sample shown in Figure 18, which is a Lambertian volume diffusor with a thickness of 2 mm, already some effect can be observed. In the figure the results of measurements are plotted in which the diameter of the measurement area on the sample was enlarged while keeping the diameter of the illuminated area constant. An increase of the BTDF value can be observed with growing field-stop diameter. Even at the largest available diameter the saturation value is not yet achieved, but the limit value can be taken from the plotted functional dependence.

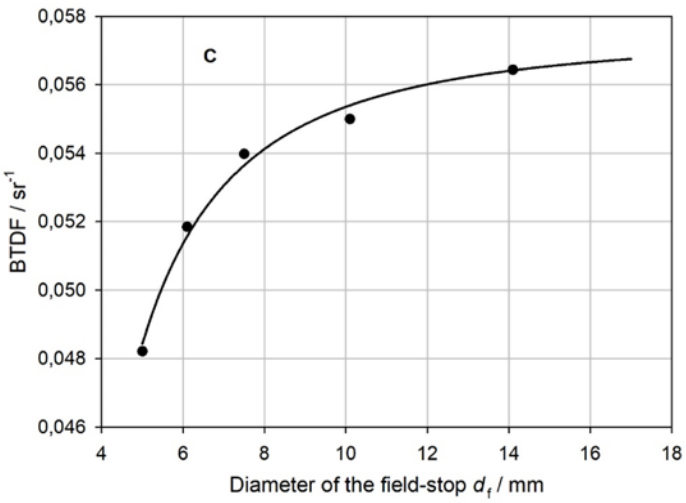

Figure 18 : Observed BTDF for a Quartz volume scatterer, measured in straight-on geometry by variation of the field-stop's diameter at constant illuminated area (d = 2.5 mm).

The size of illumination beam is an important parameter when measuring samples with dedicated surface structures. For comparable measurement results it is required to apply measurement beams with diameters $d_{beam} > d_{structure}$, choosing d_{beam} in a way that it averages several “periods” of the structure to minimize spatial inhomogeneity effects.

Speckle and interference effects should be dealt with when BTDF is measured with coherent light source. Means of reducing the coherence of illumination beam such as utilising a rotating weak diffuser should be applied to obtain more reliable BTDF results.

Diffusers used for beam manipulation and illumination purpose are often applied in the complete visual spectrum and a dedicated wavelength dependence is not desired. Typically, in the short-vis wavelength range some absorption will be found and an increase in transmittance for longer wavelengths towards near infrared range.

In Figure 19 the relative variation for five diffuser types is shown for the geometry (0°, 0° / 0° - 180°, 0°). The highest variation is found for type E, a small thickness PTFE foil. But even for this type a spectral bandwidth of about 2 nm would not cause noticeable deviation from the true value if applied in measurements.

A subtle effect can be observed for scatter angles other than Q_t = 180°. In some cases, the wavelength dependence flattens or even changes its sign when Q_t deviates from the straight-on direction. Then also the width of the scatter distribution changes slightly with wavelength. More information about this effect can be taken from [14].

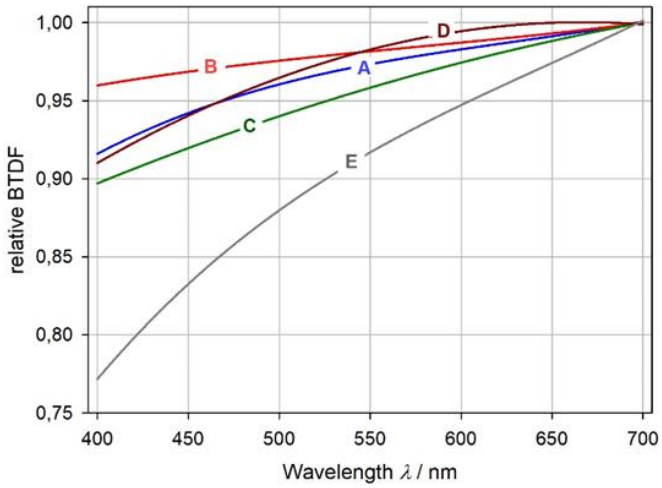

Figure 19 : Wavelength dependence of five optical diffuser types expressed as relative BTDF values for the straight-on scattering. situation A: surface treated polymer; B: fused silica ground glass; C: Quartz with air-bubbles; D: holographic plastic on glass substrate; E: thin PTFE foil.

4.3.6 Sphere-based and gonio-based transmittance haze

CI investigated the use of goniospectrophotometry to understand and improve the current sphere-based methods of measuring transmittance haze.

Transmittance haze is defined as the fraction of transmitted light that deviates from the incident beam by more than 2.5°. Various documentary standards specify the use of an integrating sphere with a prescribed geometry for the measurement of transmittance haze.

Transmittance haze can also be measured according to the definition by integrating BTDF measurements. Three samples were selected for this study. 5P-2 was a cellulose nanofibrils sample fabricated by Innventia, H5 was a holographic diffusing sample, and H2 was a nominally 0.5 mm thick piece of sintered halon, made at CI. The samples represent a range of scattering behaviour, as shown from the BTDFs measured by CI for the samples shown in Figure 20 (a). High resolution BTDF at small angles of the cellulose nanofibrils and holographic diffusing samples were also carried out by CNAM.

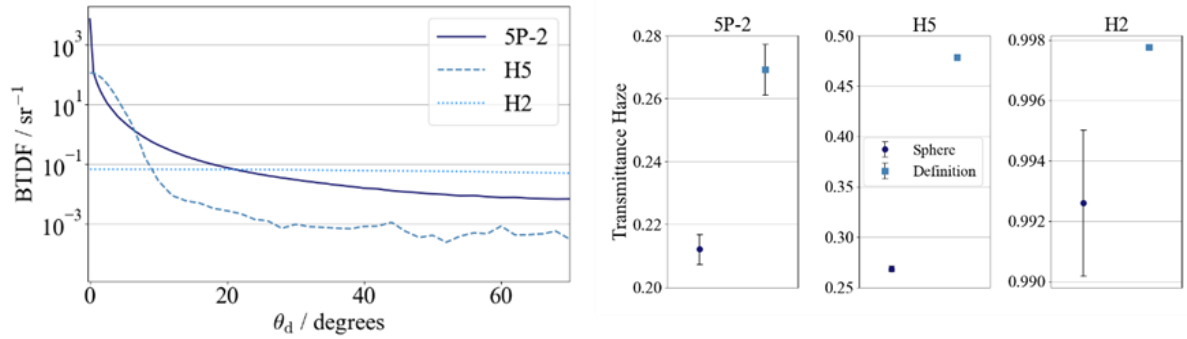

Figure 20 : (a) BTDFs of the three samples used for this work measured with normal incidence and averaged over ϕ_d. (b) haze values measured according to the definition, by integrating BTDF data, compared with haze values measured according to the ISO 14782 documentary standard. The error bars plotted show the expanded uncertainties calculated for 95% confidence.

CI calculated the transmittance haze values from their BTDF measurements and compared them to measurements using the ISO 14782 method on their integrating sphere. They found that the two results did not agree. Figure 210(b) shows the differences in the haze values for the three samples.

Upon consideration, this is not surprising. Because of the large beam size in the sphere measurements, the diffuse transmittance component meant to capture all light scattered by more than 2.5° actually includes some light scattered by only 1.3°, while some light scattered to as much as 6.7° is not included. The difference between the integrating sphere haze and the true haze (i.e., conforming to the definition and obtainable from the BTDF measurements) therefore depends on the shape of the BTDF in this range of angles.

CI also used BTDF measurements to understand sensitivity to errors in sphere geometry, which depend on the sample scattering behaviour. They showed that for some samples, the tolerances described in documentary standards can result in significant variability in the results obtained.

Like many other quantities intended to correlate with a visual perception, transmittance haze is a reduction of the full scattering distribution of a material to a single quantity. Whether this particular reduction is suitable depends on the purpose of the measurement, and the visual effect that is sought. It would be interesting to get a better understanding of the information that the various users of haze measurements require. Then, if the current sphere-based methods of realising haze are not appropriate, new measurement methods could be developed to suit the purpose of the measurements. Having these results, the project successfully achieved the objective.

4.4 Development of primary reference facilities and reference samples (artefacts) for the measurement and dissemination of the bidirectional scattering surface reflectance distribution function (BSSRDF)

BSSRDF is seen today as the ultimate quantity to characterize the optical properties of a surface or of a material. That quantity is widely used in computer graphics to generate translucency to render the appearance of skin, ceramics, or liquids. So the quantity is used and modelled, but from a metrological point of view, this field is virgin. The quantity is not defined and the mise en pratique doesn't exist.

The project addressed the challenge to set up the metrology of BSSRDF by defining the quantity, by selecting samples, by developing three independent realizations of the BSSRDF scale and by comparing these realizations together. In parallel, rendering models have been confronted to measurements for the first time.

4.4.1 Definition of BSSRDF measurand

A reportership, proposed by CSIC and CNAM, was created in CIE Division 2 as **DR 2-86 "Definitions for bidirectional scattering surface distribution function (BSSRDF)"**. The definition of BSSRDF given in this reportership is candidate to be included in the CIE International Lighting Vocabulary.

The BSSRF definition was agreed as:

Function describing the change with irradiation direction, $\mathbf{r}_i$, scattering direction, $\mathbf{r}_r$, irradiation position on surface, $\mathbf{x}_i$, and scattering position on surface, $\mathbf{x}_r$, of the quotient of the radiance of the surface element, $dL_r(\mathbf{x}_i, \mathbf{r}_i; \mathbf{x}_r, \mathbf{r}_r)$, by the directional radiant flux, $dF_i(\mathbf{x}_i, \mathbf{r}_i)$.

Fundamental scattering quantities for the determination of reflectance and transmittance

As a results from the discussion on the BSSRDF discussion, CSIC, DTU, PTB, University of Lyon and University of Poitiers proposed the definition of more fundamental scattering than BRDF and BSSRDF.

The bidirectional reflectance distribution function (BRDF) and the bidirectional scattering - surface reflectance distribution function (BSSRDF), which relate radiance at the surface to irradiance and radiant flux, respectively, are regarded as the most fundamental scattering quantities used to determine the reflectance of objects. However, for materials where the optical radiation is transmitted under the surface, this radiance depends not only on irradiance and radiant flux, but also on the size of the irradiated area of the surface. The work provides insight into such dependence under the special condition in which the radiance is evaluated within the irradiated area and, consequently, is produced by both the insurface reflection and the subsurface scattering, in contrast to the situation in which the radiance is evaluated at non-irradiated areas and only subsurface scattering contributes. By explicitly considering both contributions, two other scattering quantities are defined: one that accounts exclusively for the insurface reflection and the other that accounts for subsurface scattering. In this regard, these quantities might be considered more fundamental than the BRDF and the BSSRDF, although they are coincident with these two functions apart from the above-mentioned special condition and for materials with negligible subsurface scattering. In this work, the relevance of the proposed scattering quantities is supported by experimental data, practical considerations are given for measuring them, and their relation to the bidirectional transmittance distribution function (BTDF) [4].

4.4.2 Independent realization of BSSRDF scale

At CSIC

A primary facility for measuring the BSSRDF was developed at CSIC, based on the gonio-spectrophotometer conceived for BRDF measurements. This system is composed of three sub-systems: the irradiating system, which is fixed; the sample-positioning system, a 6-axis robot arm; and the collection system, a CCD camera on a circular rail. This design allows any irradiation and collection direction to be realized by a coordinates system transformation. A sketch of the system is shown in Figure 21.

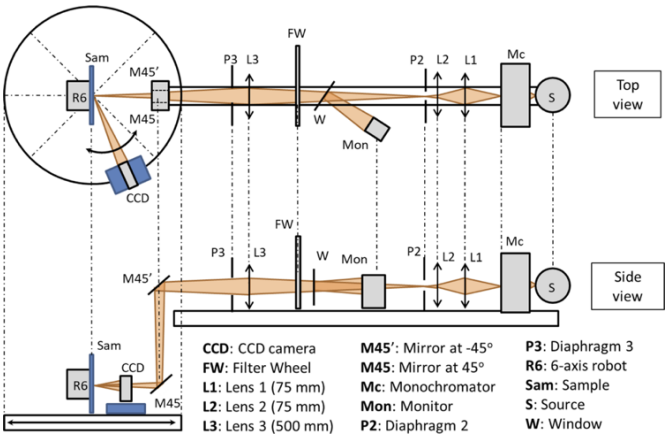

Figure 21 : Sketch of the BSSRDF measuring system developed at CSIC.

The irradiating system consists of an incandescent lamp as a light source, attached to a monochromator to provide spectral resolution. The optical system is designed to obtain a small irradiated area on the sample surface with a high irradiance, since the smaller irradiated area, the better insight into the spatial dependence of the BSSRDF is obtained. Uniformity is not needed, because the relevant quantity in the BSSRDF measurement is the incident radiant flux. A filter wheel with five different positions, i.e., clear position (no filter), dark position (opaque filter) and, 10 %, 1 % and 0.01 % transmittance-neutral-density filters, allows the irradiance to be reduced to avoid saturation in the detection system when measuring the incident radiant flux. A CCD camera is used for the detection to provide spatial resolution. The configuration of the macro lens together with the working distance provides a spatial resolution of 41.8 µm/pixel on the sample surface.

For this facility a measurement model was proposed, from the basis of the BSSRDF definition. To test the system, the BSSRDF of 12 translucent samples, with controlled values for the mean diameter of the scattering particles and their mass concentration, was measured at 40 different measurement geometries, in and out of plane. For each measurement geometry, a high dynamic range (HDR) acquisition is performed to resolve as much radiance levels as possible on the sample surface with sufficient signal-to-noise ratio (SNR). The BSSRDF results for a specific measurement geometry at an illumination wavelength of 550 nm are shown in Figure 22, where the horizontal axis represents the distance to the centre of the irradiated area.

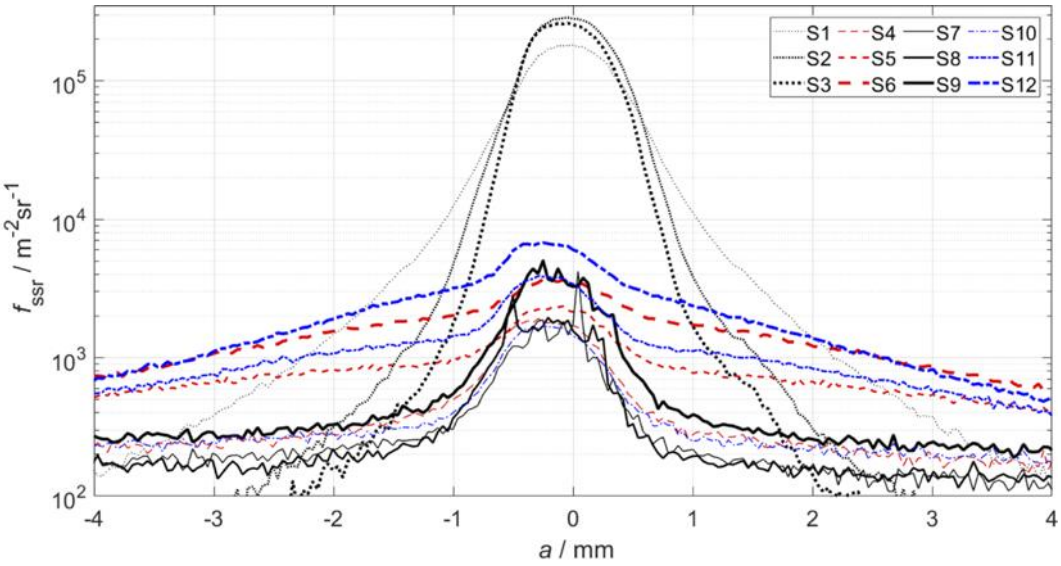

Figure 22 : BSSRDF profiles of every sample at the measurement geometry with $\phi i = 0°$, $\theta i = 15°$, $\theta r = 10°$ and $\phi r = 0°$, irradiated with $\lambda = 550$ nm.

The error sources limiting the relative standard uncertainty of the BSSRDF measurement for this facility are the response of the pixels and the responsivity ratio of the camera between reflected and incident radiant flux measurement configurations. More details about this work can be found in [5, 13].

At CNAM

CNAM developed a goniospectrophotometer for measuring the BSSRDF of samples made of translucent material. The experimental setup comprises an illumination system, a detection system placed on translation stages, a sample holder, and shares mechanical parts with CNAM's reference goniospectrophotometer. It was designed with the following criteria in mind:

- The illuminating beam and the observation area must be small, to guaranty a satisfactory spatial resolution. A poor spatial resolution would impact the measured signal like a low-pass filter, and the high frequency information (located near the illuminated area for BSSRDF measurement) would be lost.
- The incident flux must be high and the detection system must be sensitive, to measure the reflected radiance with a satisfactory signal-to-noise ratio. Indeed, outside the illuminated area, the fraction of

incident light that is collected by the detection system is very small, especially when the sizes of the illumination and observation areas are small.

- The dynamic range of the detection system must be sufficient to measure signal inside and outside the illuminated area (at least 6 decades of measurement range).

Since the objective was to build a traceable reference measurement setup, CNAM decided to build a BSSRDF goniospectrophotometer relying on a punctual measurement system combined with a spatial scanning system for the detection system, which offers an easier route for traceability than camera-based setups, at the cost of spatial resolution and measurement time. The detection system is the one used for µBRDF measurements, a CS2000 spectroradiometer (Konika Minolta) with a custom optics that allow measurements on an area of diameter 300 µm with an aperture of 1.5°. It is placed on motorized horizontal and vertical translation stages to measure the reflected radiance at various positions on the sample. The illumination system is the one used for µBRDF measurements, it creates a light beam converging on the sample plane with an aperture of 1.5° and illuminating the sample on an area smaller than 50 µm of diameter. It is placed on a breadboard that can rotate around the sample using a rotation ring, to illuminate the sample at various angles. The sample is held vertically using a 6-axis robot arm (RV 12S, Mitsubishi) and is aligned at the center of the goniospectrophotometer using the translation and rotation features of the robot arm. As the detection system is placed on a fixed optical table, the rotation ring and the rotations of the robot arm are used to orientate the source, the detection and the sample to reach the desired geometries of measurement (directions of illumination and observation).

CNAM used this setup to measure the BSSRDF of sintered PTFE (commercially known as Spectralon), a material that presents a very low translucency, visible only at small scales, as shown on Figure 23 (right). The measurement results, shown on Figure 23 (left) have been validated using numerical simulations and BRDF measurements done using CNAM's reference goniospectrophotometer: the comparison with optical simulation shows that the results have the right shape, but the comparison with the BRDF values shows that the BSSRDF order of magnitude is erroneous, mainly due to stray light in the detection system. As a full characterization of stray light to derive a correction factor is difficult, CNAM proposed to use the relation between BRDF and BSSRDF to estimate a correction factor.

However, the measurement capabilities of this setup are limited to samples of very low translucency like sintered PTFE. When the sample is of medium to high translucency, the signal-to-noise ratio is not sufficient anymore. Therefore, for the measurement of Covestro samples, CNAM replaced the CS2000 by a luminancemeter with a greater sensitivity, but a larger area of measurement.

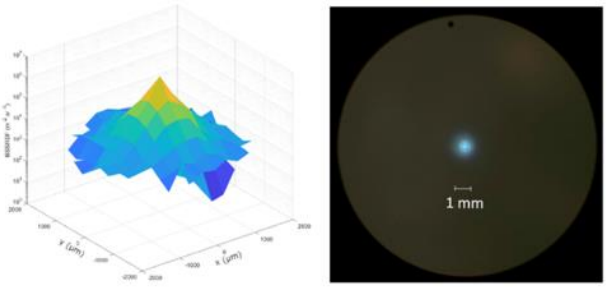

Figure 23 : BSSRDF of Spectralon measured for illumination and observation geometries of 0° and 10° respectively, shown in logarithmic scale (left) and picture of the Spectralon illuminated by CNAM's microbeam source (right).

At KU-Leuven

At KU-Leuven the Light&Lighting laboratory is equipped with a near-field goniophotometer (NFG). NFGs are normally used to determine the radiation pattern and or ray file of a light source. A NFG typically consists of a calibrated Imaging Luminance Measurement Device (ILMD) which captures luminance images as it rotates around the light source in a spherical manner. As such, it can be modified to also measure BSSRDF. The modifications to the NFG include a customized laser illumination setup and sample holder.

As light source a 4.5 mW green laser diode (type CPS532 - 4.5 mW) with a center wavelength of 532nm and circular beam shape with a diameter of 3.5 mm (at a distance of 50.8 mm) was chosen. To create a smaller and more uniform illumination spot on the sample at the center of the NFG, an aperture with a diameter of 1 mm was positioned in front of the laser. This aperture is imaged at the center of the NFG by use of a lens with a focal length of 33 cm, creating a spot size of around 2.6 mm in diameter at the sample plane. A dedicated sample holder was designed, 3D printed and attached to the NFG. The sample holder can be rotated manually to adjust the angle of incidence of the illumination beam, allowing for different measurement geometries. A live view from the ILMD, containing an overlay of the internal NFG coordinate system, is used during the alignment of the sample. First, the front surface of the sample, of which the BSSRDF is to be determined, is aligned to coincide with the center of the NFG and to be perpendicular to the illumination beam. Finally, the sample can be rotated to the desired measurement geometry.

For the determination of the BSSRDF the total incident luminous flux, on the sample is needed. As the beam is highly collimated, the standard measurement procedure of the NFG to determine the total luminous flux of light sources cannot be used. Therefore, a calibrated barium sulfate reflectance tile with a known radiance factor is introduced in the measurement system and aligned to a 0°/45° (angle of incidence/viewing angle) geometry.

To determine the BSSRDF of a sample, once it is aligned, a High Dynamic Range luminance image is captured at the desired measurement geometry. Afterwards a projective rectification is performed in order to compensate for a viewing angle which is not perpendicular to the sample (see Figure 24 left).

From both the captured luminance image of the sample and the calculated incident luminous flux, the BSSRDF can be determined. A cross section of the BSSRDF in the plane of incidence for a 0°/45° and 45°/0° measurement geometry is shown in Figure 24 right. Reciprocity is present (except for the area coinciding with the irradiation area), validating the approach and showing the necessity of a projective rectification of the 0°/45° measurement geometry.

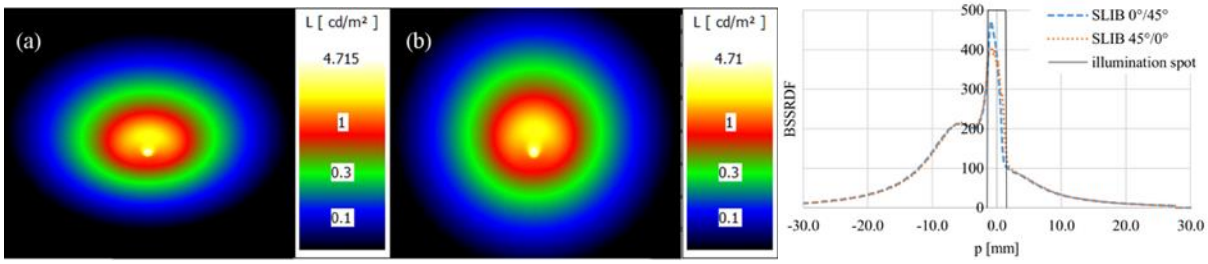

Figure 24 : Left : False color luminance image of translucent sample at a viewing angle of 45° (a) and projectively rectified (b). Right : BSSRDF values in the plane of incidence of a translucent sample for the measurement geometries 0°/45° (dashed line) and 45°/0° (dotted line) and indication of the illumination spot area (solid line).

4.4.3 Comparison of BSSRDF scales

The geometrical parameters achieved by a BSSRDF measuring system depend on the design of the system, with technical choices made to satisfy as many constraints as possible, both scientific (e.g., measurement parameters, traceability) and practical (e.g., measurement time, cost, size of the facility), with limitations caused by the complexity of the measurement. In this work, two primary facilities developed to provide traceable BSSRDF measurements are compared. One developed at the *Instituto de Óptica "Daza de Valdés"* (CSIC), the designated institute in charge of the primary references for radiometry, photometry and spectrophotometry for Spain, and another one developed at the *Conservatoire National des Arts et Métiers* (CNAM), the designated institute in charge of the primary references for radiometry, photometry and spectrophotometry for France. A third facility, developed at the Light & Lighting Laboratory of KU Leuven university (KU), is also involved in the study. The facility developed at CSIC includes two important improvements: the incandescent lamp has been replaced by a laser driven light source (LDLS) to obtain a smaller irradiated area with enough irradiance and the CCD camera has been replaced by a high sensitivity CMOS camera with a better spatial resolution.

The objective of this study is to demonstrate that these BSSRDF measurements have traceability to the International System of units (SI) and to establish a preliminary BSSRDF scale to be transferred to the measuring system developed at KU. This work also gives us the opportunity to better understand the impact of the parameters of our facilities on the BSSRDF measurement according to the translucency and surface properties of the measured sample.

The results on the comparison between CSIC and CNAM measurements of the BSSRDF of three translucent samples (A, B and C from most opaque to most transparent, respectively) at three different in-plane geometries are shown in Figure 25, where no results are shown from CNAM for sample C since its measurements on this sample were too noisy, due to the high transparency of the sample.

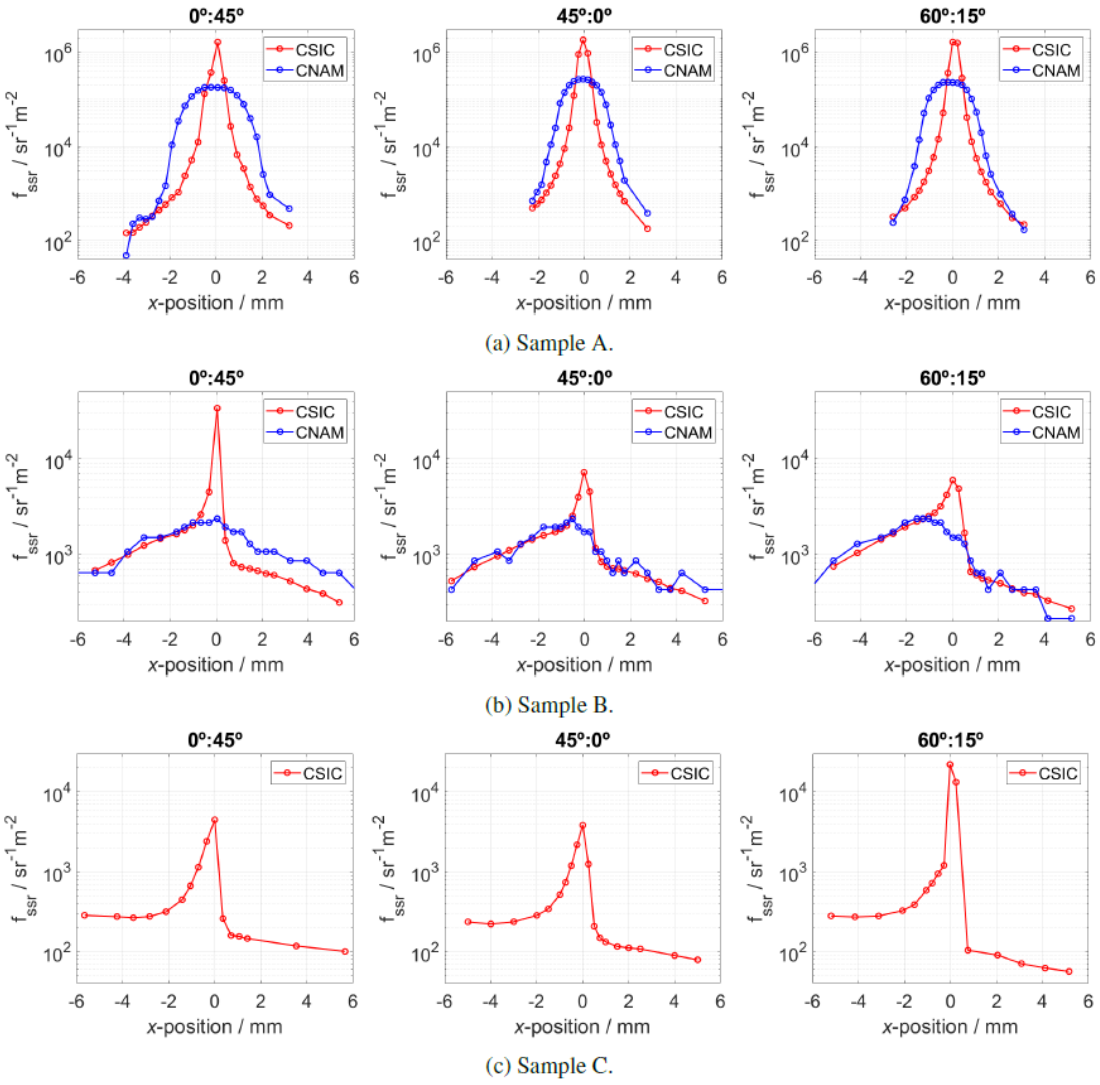

Figure 25 : Measured BSSRDF values of three translucent samples at CSIC (red) and CNAM (blue).

Due to the high uncertainty of CNAM measurements, it was decided to consider the measurements at CSIC as the better estimation of the BSSRDF. The results obtained with the system developed at KU on sample B at the same measurement geometries are shown in Figure 26, in comparison with CSIC measurements.

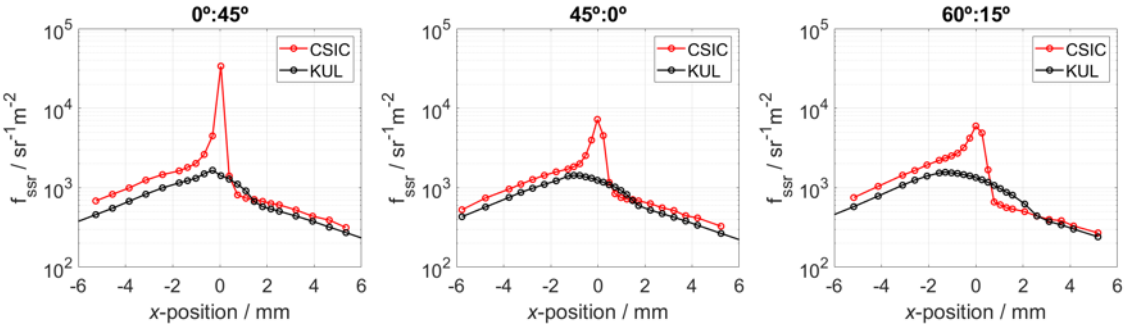

Figure 26 : Measured BSSRDF values of the sample B at CSIC (red) and KU (black).

The BSSRDF scale realized by two different measurement facilities (at CSIC and CNAM) has been compared through the measurement of three samples with different levels of translucency specifically produced for this study. The measurements on samples A (the opaquest) and C (the most transparent) need a very high sensitivity of the detection systems, since most of the reflected radiant flux is within or very close to the irradiated area, hiding the effect of scattering in the bulk. The BSSRDF measurements of those samples allowed the complexity of the measurement to be understood for such extreme cases. For a more intermediate case, as the translucent sample B, the BSSRDF measurements showed a good agreement between the two facilities.

In addition, the BSSRDF scale has been transferred to the BSSRDF measuring system at KU. The relative values of the BSSRDF measurements at KU agree well with the previously obtained values from the comparison between CSIC and CNAM, and a calibration factor for this facility was obtained. We observed some dependence of this calibration factor on the geometry and on the position on the sample, which might be a consequence of the different realization of the bidirectional geometry and the size of the irradiated area.

Finally, some recommendations can be given for the appropriate selection of the detection system for different purposes of the BSSRDF measurement. A camera-based system should be more adequate for industrial applications, as it can provide BSSRDF measurements faster than using a detector without spatial resolution. In addition, we have shown that, although a conventional system based on a calibrated luminance meter might be used for providing traceability at very specific conditions, a camera-based system can be used for metrological applications too.

4.4.4 BSSRDF measurements and models

The radiative transfer equation (RTE) provides an efficient way of modelling light propagation through materials exhibiting volumetric scattering. To simulate light propagation through a specific scattering material, the RTE requires three parameters. The first two, the scattering and absorption coefficients, s_s and s_a, define the proportion of light redistributed due to scattering and absorption, respectively, per path length. The third parameter is the single-scattering phase function, $p(\theta)$, which describes the angular redistribution at each scattering event. In other words, at every scattering event the phase function defines the probability of each new direction that the light ray can take. The phase function can take an arbitrarily complex shape, but in practice some simplifications are typically employed. In most cases in lighting, the scattering is assumed to be rotationally symmetric, which is generally true for non-birefringent samples with random orientation of the scattering particles. Furthermore, in most cases a phase function model is used, which permits defining the phase function with a single parameter (g) or a small set of parameters. Simulation of light transport in flat, thin scattering volumes placed on grid paper are illustrated in Figure 27.

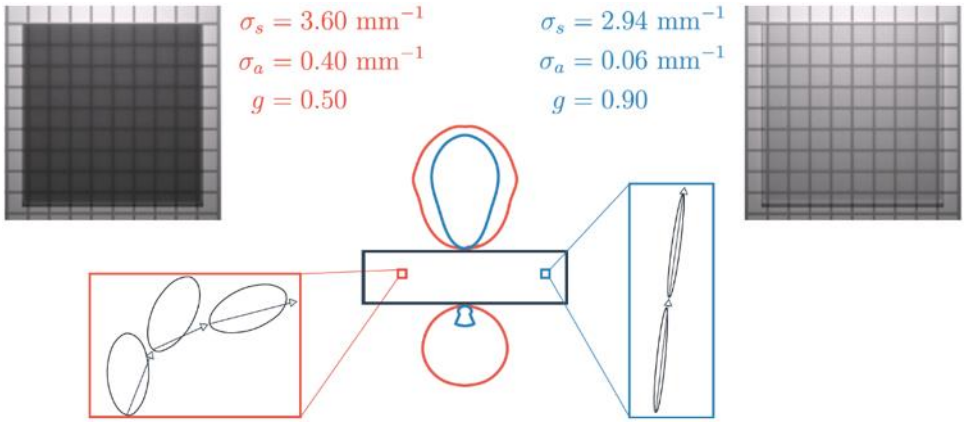

Figure *27*: Renderings of flat samples (1 mm thick) placed on grid paper and illuminated from above. The samples have the listed scattering properties, which result in the plotted radiant intensity distributions for light incident from below the sample. The inserts illustrate the effect of the phase function. Information from a measured radiance distribution can improve the accuracy of estimated scattering properties as compared to using a measured radiant intensity distribution or only the total reflection and transmission.

In the inverse approach, it is not necessary to know the microscopic scattering properties or particle geometry. Instead, the macroscopic properties are estimated directly from experimental measurements of the behavior of light when it interacts with the sample. Change in the behavior of light is used to predict the scattering properties of the sample. An inverse approach requires measurements of the light scattered by a sample and a method to simulate how the sample scatters light. The above-mentioned measurements provide one way of meeting the first requirement. Methods such as Monte Carlo ray tracing and adding-doubling are usually available to simulate scattered light from samples when their volume scattering parameters are known. Having met the two requirements, the inverse approach is usually framed as a numerical optimization problem. The goal is to find the set of scattering model parameters that minimizes the difference between the simulated and experimentally measured scattered light distribution. Depending on the numeric tool used to simulate the scattered light distributions, the inverse method takes a different name. Inverse adding-doubling (IAD) and inverse Monte Carlo use the adding-doubling method and the Monte Carlo ray-tracing method, respectively, to perform the simulations. Depending on the method chosen to perform the simulations, it may be necessary to carefully consider which numerical optimization method is best suited for the inverse problem.

We have investigated the capabilities of the inverse adding-doubling method in extracting accurate and robust volume scattering properties from experimental measurements of scattering material samples. The scattered radiant intensity for several different samples was measured, and inverse adding-doubling was applied to estimate their corresponding volume scattering properties, resulting in good matches between simulations and experiments (see Figure 28). To assess the robustness of the scattering parameters estimated with inverse adding-doubling, samples with higher concentration of scattering particles and multiple types of scattering particles were also measured but not subjected to inverse adding-doubling. Instead, the properties previously estimated were used directly with adding-doubling to simulate the scattered radiant intensity, and this was compared to experimental measurements. An overall good match between experiments and simulations was found for both tests, demonstrating that inverse adding-doubling is capable of estimating the volume scattering properties of samples in an accurate and robust manner. Having these results, the project successfully achieved the objective [1,3].

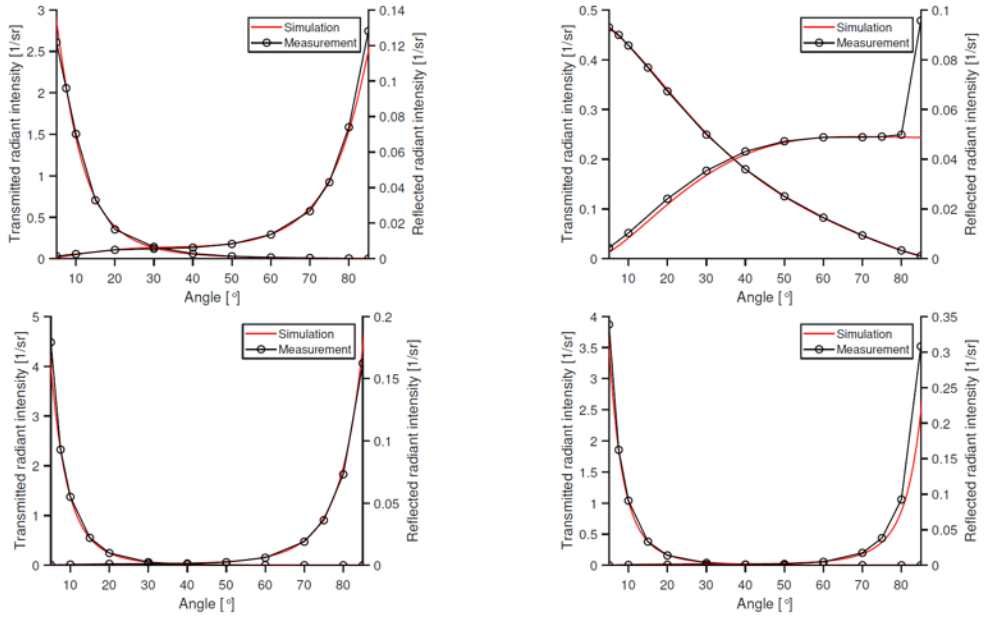

Figure *28* Comparison between measured and simulated scattered radiant intensity for the (left) best match and (right) worst match. The top and bottom rows show results for two different materials.

5 Impact

The project website, which is hosted by CMI, has had almost 20,000 visits over the period of the project. Five progress meetings have been organized during the project that had on average 50 attendees including 60 % of industrial stakeholders from different sectors, e.g. pigments, spectrophotometer manufacturers, pulp & papers, automotive or cosmetics.

Fifteen publications have been published (or approved for publication) in peer reviewed journals. Four additional papers are still under review. Outputs of the project have been presented at 14 international conferences and 11 national conferences in France, Germany and Spain. Among these 24 presentations, 3 were invited talks. Members of standardisation groups (CIE, DIN, DfwG and ISO/TC6) have given 22 presentations during progress or annual meetings to inform members about the project launch and results.

Due to the pandemic, workshop on BTDF measurement, on speckle and on Models had to be postponed to the end of the project but could be done (respectively on Apr 22, Dec 21 and Sept 22).

Impact on industrial and other user communities

The field of spectrophotometry is evolving quickly, and new commercial devices are continuously coming to the market. The appropriate characterisation and calibration of all these different types of goniospectrophotometers requires a coordinated effort between European NMIs. Thanks to the project, the consortium is now able to provide BTDF calibration services to manufacturers of novel spectrophotometers, R&D industries and others. The effect of speckle is better known which has an impact on the calibration of glossmeters.

The reduction of the BRDF measurement uncertainty and the validation and improvement of BRDF scales reduces the uncertainty of the calibration for spectrophotometer manufacturers, which has an immediate effect at the industrial level.

The definition and realisation of BSSRDF scale has been done and will have a direct impact on different industries e.g. cosmetics, automotive, plastics, pulp and paper as well as on rendering software developers as it will provide the calibration solution for devices that have already been developed. Even if the uncertainty still needs to be decreased for this quantity, the first applications tested on existing models have allowed to better understand the limitations of the models, and the optical properties of translucent materials.

Impact on the metrology and scientific communities

Progress in the comprehension of the effect on light coherence in BRDF measurement with narrow spectral bandwidth and/or hight angular resolution have a direct impact on the scientific community because it questions the notion of BRDF itself. The work done to define the measurand for BRDF and BSSRDF has an

impact for manufacturers of spectroradiometer, particularly for those who are developing image-based devices. Better control of BRDF leads to reduced Calibration and Measurement Capability (CMC) uncertainties at several participating NMIs, therefore improving the quality and the visibility of European metrology in the field of spectrophotometry. This work is already engaged with publication of papers claiming this reduction of uncertainties (see here). New primary facilities for the measurement of BTDF, BSSRDF and µBRDF have been constructed at several NMIs and will lead to new calibration services at NMIs. An important work of collaboration has been engaged with stakeholders to develop of new Certified Reference Materials (CRM), which will make traceability of BRDF, BTDF and BSSRDF more accessible to the European metrology community.

Impact on relevant standards

This project focused on the improvement and development of traceable quantities for the characterisation of the visual and optical properties of materials, which forms the terms of reference of CIE Division 2. The project impacted the work carried out in several CIE technical committees such as CIE TC2-85 (normalisation on BRDF), CIE JTC12 (measurement of sparkle and graininess) and CIE JTC17 (measurement of gloss). A reportership on the definition of BSSRDF has been opened by CIE (DR 2-86). Thanks to it the CIE international vocabulary has been extended by the project through the definition of BSSRDF. International metrology committees such as CCPR and EURAMET-TC-PR has been periodically informed about the progress of BxDiff. New calibration and measurement capabilities (CMCs) will be submitted on BTDF in short term and on BSSRDF on a longer term. As a consequence of this project, normalisation work on the measurement of BTDF and BSSRDF is foreseen.

Longer-term economic*, social and environmental impacts*

By providing new and reliable metrological references in spectrophotometry, this project improves the quality control of the appearance of objects and its virtual reproduction. The control of appearance is directly linked to the success and the competitiveness of goods. The project leads to improved rendering models able to better simulate the appearance of complicated objects. The uptake of outputs of the project will benefit computer generated imagery in movies and video games, digital prototyping of products, skin appearance rendering for medical and cosmetic industries, 3D printing, and energy assessment of buildings with glazing materials.

6 List of publications

1. A. Correia, P. Hanselaer, Y. Meuret, 2019, “Accurate and robust characterization of volume scattering materials using the intensity-based inverse adding-doubling method”, SPIE Vol 11057, https://lirias.kuleuven.be/2825988?limo=0
2. A. Calderón, A. Ferrero and J. Campos, 2020, “Accounting for polarization–related effects in the measurement of the bidirectional reflectance distribution function”, Metrologia 57(4), https://iopscience.iop.org/article/10.1088/1681-7575/ab804f
3. J. R. Frisvad, S. A. Jensen, J. S. Madsen, A. Correia, L. Yang, S. K. S. Gregersen, Y. Meuret, P.-E. Hansen, 2020, “Survey of Models for Acquiring the Optical Properties of Translucent Materials”, Computer Graphics forum (39)2, pp 729-755, https://diglib.eg.org/handle/10.1111/cgf14023
4. A. Ferrero, J. R. Frisvad, L. Simonot, P. Santafé, A. Schirmacher, J. Campos, and M. Hebert, 2021, Fundamental scattering quantities for the determination of reflectance and transmittance“, Optics Express 29(1), https://www.osapublishing.org/oe/fulltext.cfm?uri=oe-29-1-219&id=445047
5. P. Santafé-Gabarda, A. Ferrero, N. Tejedor-Sierra and J. Campos, 2021, “Primary facility for traceable measurement of the BSSRDF”, Optics Express 29(21), pp. 34175-34188, https://doi.org/10.1364/OE.439108
6. I. Santourian, T. Quast and A. Schirmacher, 2022, Uncertainty budget for PTB's gonioreflectometers and ways to improve it in the short VIS spectral range, Metrologia 59(2), https://iopscience.iop.org/article/10.1088/1681-7575/ac4e76
7. T. Labardens, P. Chavel, Y. Sortais, M. Hébert, L. Simonot, A. Rabal, G.Obein, 2021, Study and simulations of speckle effects on BRDF measurements at very high angular resolution, Electronic Imaging, 33, https://library.imaging.org/ei/articles/33/5/art00006

8. I Santourian, T Quast, S Teichert, K-O Hauer and A Schirmache, 2022, Novel LED-based radiation source and its application in diffuse reflectometry and polarization measurements, J. Phys.: Conf. Ser. 2149 012010, https://doi.org/10.1088/1742-6596/2149/1/012010
9. P. Chavel, Y. Sortais, T. Labardens, L. Simonot, M. Hebert, G. Obein, 2022, Advocating a statistical definition for the BRDF, Journal of Physics: Conference Series, 2149. https://hal-universite-paris-saclay.archives-ouvertes.fr/hal-03620283/
10. Z. Ma, P-E. Hansen, H. Wang, M. Karamehmedovic, Q. Chen, 2023, Harvey-Shack theory for converging-diverging Gaussian beam, JOSA B, https://doi.org/10.1364/JOSAB.478801
11. E. Molloy, P. Saunders, A. Koo, Effects of rotation errors on goniometric measurements, 2022, Metrologia, 59(2). https://zenodo.org/record/5842491
12. N. Basic, E. Molloy, A. Koo, Al. Ferrero, P. Santafé, L. Gevaux, G. Porrovecchio, A. Schirmacher, M. Smid, P. Blattner, K-O. Hauer, T. Quast, J. Campos-Acosta, G. Obein, 2023, Intercomparison of bidirectional reflectance distribution function (BRDF) measurements at in- and out-of-plane geometries, Applied Optics, https://opg.optica.org/ao/upcoming_pdf.cfm?id=486156
13. P. Santafé, 2020, Medida y transferencia de la unidad de BSSRDF, Master Thesis, Spain, https://digital.csic.es/handle/10261/226200.
14. J. Fu, J.Reval F., M. Esslinger, T. Quast, A. Schirmacher 2022. Preliminary Results of Angle-Resolved BTDF Characterization of Optical Transmissive Diffusers, Colour and Visual Computing Symposium 2022 (CVCS 2022). Identifier: urn:nbn:de:0074-3271-0, https://ceur-ws.org/Vol-3271/Paper13_CVCS2022.pdf
15. J.S.M. Madsen; R. Korhonen; P. Peltonen; O. Rodenko; S.A. Jensen. Nanostructure characterization and film thickness measurements at the fabrication line. “Nanomaterials: Applications & Properties” (IEEE NAP-2022), Krakow, Poland, Sep. 11-16, 2022. https://doi.org/10.5281/zenodo.7973545